5-2007

Geochemical modeling of solubility and speciation of uranium, neptunium, and plutonium

Zhongbo Yu

Yuyu Lin

Karen Johannesson

Amy J. Smiecinski
University of Nevada, Las Vegas, smiecins@unlv.nevada.edu

Klaus J. Stetzenbach
University of Nevada, Las Vegas, STETZENB@unlv.nevada.edu

MODEL COVER SHEET

Complete only applicable items

☒ (1) Model Check all that apply:

Type of Model

- ☐ Conceptual Model
- ☐ Mathematical Model
- ☒ Process Model
- ☐ Abstraction Model
- ☐ System Model

Intended use of Model

- ☒ Input to Calculation
- ☐ Input to another Model
- ☐ Input to Technical Document
- ☐ Input to other Technical Products

Describe use:

This model is used to evaluate the sensitivity of the current models to solubility data and to predict the impact of actinide speciation data on the behavior and mobility of actinide species.

(2) Title: Geochemical Modeling of Solubility and Speciation of Uranium, Neptunium, and Plutonium

(3) Document Identifier (including Revision No.): MOD-06-001

(4) Total Attachments: 1		(5) Attachment Numbers-Pages in each: 8 pages	
	Printed Name:	**Signatures:**	**Date:**
(6) Originators	Zhongbo Yu and Yuyu Lin	[redacted]	23 May 2007 24 May 2007
(7) Technical reviewer	Karen Johannesson	[redacted]	21 May 2007
(8) QA Manager	Amy Smiecinski	[redacted]	24 May 2007
(9) Principal Investigator	Klaus J. Stetzenbach	[redacted]	24 May 07

(10) Remarks:

MODEL REVISION HISTORY

Complete only applicable items

(2) Model Title:

Geochemical Modeling of Solubility and Speciation of Uranium, Neptunium, and Plutonium

(3) Document Identifier (including Revision No.):

MOD-06-001 REV 00

(4)	(5) Description of Revision
0	**Initial Issue**

ACRONYMS

ACC	Yucca Mountain Project Records Accession Number
AMR	Analysis Model Report
DIRS	Document Input Reference System
DOE	U.S. Department of Energy
DTN	Data Tracking Number
ESF	Exploratory Studies Facility
NRC	U.S. Nuclear Regulatory Commission
NCEWDP	Nye County Early Warning Drilling Program
NTS	Nevada Test Site
OCRWM	Office of Civilian Radioactive Waste Management
Q	Qualified
QA	Quality Assurance
QAP	Quality Assurance Procedure
RW	Radionuclide Wastes
RWP	Radionuclide Wastes Package
SZ	Saturated Zone
UQ	Unqualified
USGS	U.S. Geological Survey
UZ	Unsaturated Zone
YM	Yucca Mountain

TABLE OF CONTENTS

LIST OF TABLES

LIST OF FIGURES

1. PURPOSE

The purpose of this study is to model the solubility, speciation, and transport of three actinides: uranium (U), neptunium (Np), and plutonium (Pu) by a geochemical modeling tool under possible repository environmental conditions upon waste package failure. The dissolution concentration of three actinides in the waste package, their aqueous speciation after dissolving in the unsaturated zone (UZ), and transport processes in the saturated zone (SZ) along the groundwater flow path at Yucca Mountain (YM) are simulated by geochemical modeling calculations using PHREEQC. This model report was prepared in fulfillment of *Groundwater Characterization at Yucca Mountain, Task II: Surface Complexation and Solid Phase Dissolution*, *Subtask 6: Phenomena Modeling of Actinide speciation simulation* (Research Foundation Task: ORD-RF-02). This subtask with evaluates of the sensitivity of the current models to solubility data and impact of actinide speciation data on the behavior and mobility of actinide species. For fundamental theory of three concerned actinide species on which the simulation built up, please see Technical Report, "Groundwater Characterization at Yucca Mountain, Task 2: Surface Complexation and Solid Phase Sorption" (Czerwinski, 2007).

Uranium, neptunium, and plutonium have been considered to be the most important components in high-level radionuclide wastes (RW) after hundreds of years deposit. The geochemical model includes three sub-models: solubility model, aqueous speciation model, and transport model. Three actinides are programmed separately in each sub-model. According to the definition of unqualified data, the third sub-model uses some unqualified data, so the modeling results of transport are considered to be Unqualified (UQ) and are not included in any conclusions.

The scope of this model report is to describe the development of a geochemical model for simulating dissolution concentration of three actinides in the waste package, aqueous speciation in UZ directly below the repository, and transport in groundwater system. The three sub-models include: the solubility model, where water may have seeped into the repository from the surrounding rock, percolated into a failed waste package, and reacted with the waste form in the waste package. The second sub-model is the aqueous speciation model, where the dissolved radionuclide-bearing solution exits the waste package via advection and then mixes with pore water in the UZ. The third sub-model is the transport model, where the dissolved radionuclide minerals migrate through the UZ, enters the SZ beneath the groundwater table, and then reaches the 20 km alluvium aquifer down gradient to the southwest of YM. The transport sub-model involved some UQ data; however, the results that come from it are listed only in the Appendix.

Source of data for this study are derived from YM Databases, including mineralogy, kinetics, and thermodynamics, which are valid for temperatures up to 100 ^{o}C and ionic strength up to 1 molal.

2. QUALITY ASSURANCE

QA Program Applicability: The model was developed in accordance with the Nevada System of Higher Education (NSHE) Quality Assurance (QA) program requirements, as indicated in the Scientific Investigation Plan (SIP) (No. SIP-UNLV-045). The report contributes to the analysis and modeling data used to support the experiment results; the conclusions do not directly impact engineered features important to safety.

3. COMPUTER SOFTWARE AND MODEL USAGE

The software used in this analysis includes:

- PHREEQC V. 2.3 (10068-2.3-00 for LINUX, 10068-2.3-01 for WINDOWS 2000), a hydrogeochemical transport model by Parkhurst and Appelo (1999). This is a qualified software on Windows 2000 operating system. It is appropriate for the application and is used only within the range of validation in accordance with QAP-3.2, "Software Management." Input data sets were prepared for various simulations according to the PHREEQC input formats.

- Microsoft Excel 2000, a commercially available spreadsheet software package: Applications of this software in the current document are restricted to tabulation, visual display of results, and use of intrinsic functions (SUM, LOG, MAXIMUM, MINIMUM). No macros or software routines were developed for, or used by, this software, and consequently it is an exempt software application in accordance with QAP-3.2, "Software Management."

The simulations with PHREEQC V. 2.3 were executed on the following machine using the Microsoft Windows 2000 operating system:

- A Dell, Power Edge SC1420, Dell Inc. Tag# 2055159 in Room 117, Lily Fong Geoscience at Department of Geoscience, University of Nevada, Las Vegas.

Electronic Management of Data: Origination of data and daily documentation of this work may be found in Scientific Notebook (UCCSN-UNLV-087, volume 3). Models developed for any purpose other than the sensitivity assessment of the extant models will be developed, documented, and validated subject to QAP-3.3, "Models." The details of modeling work on the speciation simulation of actinides are documented in the scientific notebook, with electronic data and models stored subject to the requirements set forth in QAP-3.1, "Control of Electronic Data," during modeling and documentation.

4. INPUTS

4.1 DATA AND PARAMETERS

This section provides documentation for data used as inputs to this Model Report. The inputs to the modeling activities described in this Model Report are obtained from the Technical Data Management Systems (TDMS) and include the following:

- Geochemistry data from the ESF and UZ boreholes.
- Thermodynamic data of selected radioactive elements.

4.1.1 Direct Inputs

Source DTNs used in this model report for the simulation of solubility and speciation are summarized in Table 4-1. Compositions of solution used in models are listed in Table 4-2. All sources of direct inputs for these parameters are listed in Tables 4-1 and 4-2; other DTNs and data sources discussed in this section are presented for corroborative or informational purposes only.

The inputs into the solubility sub-model include chemical components of percolating water that seeped into the failed waste package, secondary minerals or alternative phases of uranium, neptunium, and plutonium as equilibrium phases, and related chemical reaction with thermodynamic data from the YM database. The outputs from the solubility sub-model include concentrations of dissolved total actinides changing with pH value as well as partial CO_2 pressure. Also the outputs include saturation indices for each selected secondary mineral or alternation phase before and after dissolution.

The construction of speciation sub-model is based on the solubility sub-model. Besides the information from the solubility sub-model, the inputs of aqueous speciation sub-model include the solution from the waste package, chemical components of UZ pore water, and the mixing of these two. The outputs from the aqueous speciation sub-model include concentrations of various aqueous species of dissolved radionuclide-bearing minerals under corresponding pH value, ionic strength, and secondary mineral abundance.

All the important inputs for this study used for PHREEQC calculations are summarized in Tables 4-1 and 4-2. The location of wells mentioned in Tables 4-1 and 4-2 are plotted in Figure 6-2 in Section 6.3. Because all thermodynamic data were chosen at 25 ºC with corresponding pressures of 1 atm (1.013 bar), no extrapolation of those equilibrium constants to higher temperatures are needed, which eliminates the major uncertainties for aqueous species as well as solids when using the database MO0312SPATDMIF.000.

Table 4-1. Input Data Source and Data Tracking Number for Solubility and Speciation Model.

Source	Data/Parameter Description
Thermodynamic Data	
SN0504T0502404.011	Pitzer thermodynamic database including actinides and transition metals
SN0302T0510102.002	Same as above
MO0312SPATHDMIF.000	Thermodynamic database for partial uranium, neptunium, and plutonium secondary minerals
Geochemistry Data of Groundwater	
MO0005PORWATER.000	Average of Tptpmn pore-water analyses ESF-HD-PERM-2 and ESF HD-PERM-3
GS000608312271.001	Pore-water hydrochemistry and isotropic data for borehole UZ #16

Table 4-2. Chemical Compositions of Solution Used in Solubility and Speciation Models.

	Solution I [a]	Solution II [b]
Description	UZ pore water above repository (from ESF-HD-PERM-2 and ESF HD-PERM-3)	UZ pore water below repository (from UZ #16)
Na^+ (mg/L)	61.5	72.5
Ca^{2+} (mg/L)	101	22
Mg^{2+} (mg/L)	17	8.4
K^+ (mg/L)	8.0	N/A
Cl^- (mg/L)	117	44.2
SiO_2 (mg/L)	70.5	62.1
HCO_3^- (mg/L)	200	171
SO_4^{2-} (mg/L)	116	23.6
NO_3^- (mg/L)	6.5	21.7
F^- (mg/L)	1.0	N/A

a DTN: MO0005PORWATER.000
b DTN: GS000608312271.001

4.1.2 Indirect Inputs

Indirect inputs are summarized in Table 4-3. These indirect inputs were utilized to evaluate uncertainties in the solubility, speciation, and transport models, or to establish the ranges of environmental conditions for calculations, or to validate the sub-models.

Table 4-3. Summary of Indirect Inputs

Entry Number	Input	Source Used In
Uncertainties in Thermodynamic Data	Lemire (2001), Tables 3.1, 3.2, 4.1, and 4.2,	Sections 6.8 and 6.9 for uncertainties in plutonium, Np_2O_5, and PuO_2 solubility models
Plutonium Solubility	Efurd et al. (1998), Table 4; Nitsche et al. (1993), Table XVI	Section 6.9 to validate the plutonium solubility model
Neptunium Solubility	Efurd et al. (1998), Table 6 Nitsche et al. (1993), Table VI	Section 6.8 to validate the Np_2O_5 solubility model
Uranium Solubility	Lemire and Tremaine (1980)	Section 6.7 to validate the uranium solubility model;

4.2 CRITERIA

Not applicable in this model report.

4.3 CODES AND STANDARDS

No specific, formally established standards have been identified as applicable to this analysis and model.

5. ASSUMPTIONS

Development of methodology for the geochemical modeling of solubility and speciation of actinides in waste package as well as porous media in the UZ, calculation of mineral–water reactions, and speciation reactions of aqueous species are discussed in Section 6. Many simplifications and approximations underlie this methodology.

The geochemical model simulates the percolating water that may seep into the repository from surrounding geological substance, enters a failed waste package, reacts with the actinides, and then exits the waste package. Firstly, nuclear wastes in the disposal repository contact the percolating water intruding into the waste package for a sufficient time to make the dissolution reaction reach equilibrium. Based on this assumption, the heat effect on the dissolution is negligible. Secondly, the solution of dissolved minerals mixes with UZ pore water. The pores of UZ are partially filled by water, so the solution transport through UZ will take a very long time. The aqueous speciation reaction can reach equilibrium under this time scale.

All calculations were made at 25°C. To estimate the effects of changing temperature on dissolution concentration, uranium calculations were made over a range of 25-50°C at a single partial pressure of CO_2. The predicted highest temperature within the RWP is up to 146 °C. There is no thermodynamic data at such ultimate temperature for uranium available in YM databases. Thus, the range of simulated temperature is set to be 15~50 ºC based on data availability. Also, there is no suitable thermodynamic data are available for the calculation of temperature effect of neptunium and plutonium.

The redox condition of repository is assumed to be oxidizing in order to be conservative. The partial pressure of oxygen is set up to be 0.2 bar (atmospheric value). Because the existence of reducing condition has not been proven except for transient and localized conditions, this is a reasonable assumption as well as conservative assumption since most actinides are either more soluble under such oxygen partial pressure or insensitive to it (OCRWM, 2003a; Runde et al., 2002).

The validation results provided by Mitcheltree (2006) about PHREEQC outputs are accepted and accurate enough for the purpose of this usage.

6. MODEL

6.1 MODEL OBJECTIVES

This study focuses on the solubility and speciation reactions of three actinides in waste package and UZ, respectively.

The objectives of this modeling effort are to (1) achieve better understanding about the chemical properties of the three actinides (^{239}Pu, ^{237}Np, and ^{238}U); (2) calculate the saturation index (SI) of radionuclide-bearing minerals to investigate its sensitivity and how concentrations of dissolved actinides change as the initial input contaminant concentration into the groundwater; and (3) determine the chemical reactions with reasonable thermodynamic data and calculate aqueous speciation of dissolved actinide-bearing species.

6.2 OVERVIEW OF THE MODEL

This section presents the concepts implemented for the development of the geochemical model. The components of the conceptual model are listed as follows: (1) percolating water penetrates into RW packages and dissolves some of the actinides. The dissolved actinides undergo re-precipitation and re-dissolution through the canisters and form a series of complex alteration phases or secondary minerals. (2) Some of these phases finally leave the waste packages and then enter the UZ. (3) During the migration through the UZ, the dissolved actinides species lead to a series of chemical reactions, such as hydrolysis reaction, and reaction with carbonate over a range of pH values.

6.3 TECHNICAL ISSUES IN SOLUBILITY EVALUATION

There are two prerequisites to solubility evaluations (OCRWM, 2003a). First, a thermodynamic database is needed along with a compatible geochemical modeling tool. Second, the environmental conditions for which solubility is to be evaluated must be defined. With these prerequisites, a model is constructed based on the environmental information and chemical properties of selected actinidess using the geochemical modeling tool. The percolating water intrusion into waste package is selected from ESF-HD-PERM-2 and ESF HD-PERM-3 (BSC, 2005). The composition of the solution is listed in Table 4-2.

The first prerequisite is input to this analysis and is discussed in Section 4.1. The second prerequisite is discussed in Section 6.4. The discussion of this section will focus on several technical issues common to the solubility evaluation, such as the definition of solubility, the selection of solubility-controlling solids, and uncertainty treatment. Specific issues related to certain elements will be discussed in relevant sections.

6.3.1 The Definition of Solid Solubility

From the viewpoint of laboratory chemistry, solubility is defined as the concentration of a substance when the solution is saturated with that substance (Atkins, 1994). In other words, solubility is the concentration of a substance when the substance is at equilibrium (either stable or metastable) with the solution. For this case, the substance is a radionuclide-bearing solid. In practice, radionuclide-bearing minerals are always used to evaluate solubility (OCRWM, 2003b). Among several available radionuclide-bearing minerals in RWP, one has a relative large composition as well as least solubility is defined as solubility-controlling solid.

Except for colloidal and kinetically transient phenomena such as over-saturation, solubility is "the maximum quantity of one phase dissolved by another under specified conditions. In the case of solutions of solids or liquids in liquids, the solubility is usually expressed as the weight (or mass) dissolved in a given weight (mass) or volume of the solvent at a specified temperate." (Sharp, 1990) and a solubility-controlling mineral phase will set the limits.

An important criterion to evaluate the solution equilibrium is saturation index (SI), which is defined as the logarithm of the quotient of the ion activity product (IAP) and solubility product constant (K_{sp}). The IAP is calculated from activities that are calculated from analytically determined concentrations by considering the ionic strength, temperature, and complex formation. The solubility product is derived in a similar manner as the IAP, but using equilibrium solubility data corrected to the appropriate water temperature (Merkel and Planer-Friedrich, 2005). The equation of SI is defined as:

$$SI = \log \frac{IAP}{K_{sp}}$$

where IAP is ion activity product, and K_{sp} is solubility product constant.

6.3.2 Uranium-bearing Mineral Solubility

To evaluate the solubility of the relevant uranium-bearing mineral within a repository, one has to identify the controlling solid or solids. Since solubility depends strongly on the solid phase, the outcome would be quite different (orders of magnitude), if different solids are chosen. From the viewpoint of thermodynamics, the most stable solid, as the controlling phase should be selected, because thermodynamically less stable phases would be finally replaced by the most stable phase. Uranium oxide is thermodynamically unstable in the presence of moisture and oxidized environments. The dissolution of uranium oxide depends on uranyl ions UO_2^{2+} or uranyl complexes such as $UO_2(CO_3)_2^{2-}$ (Murphy and Shock, 1999).

The dissolution reactions were examined in many tests conducted by Argonne National Laboratory (Wronkiewicz and Buck, 1999). An experiment which lasted eight years on the UO_2 sample indicates that about 95% of the uranium species released from a waste

package during the corrosion of the sample had subsequently precipitated back onto the sample surface, tested container, or in the corroded intergrain boundary regions. Most commonly uranium occurred in the form of dehydrated schoepite (UO_3H_2O). This phase only consists of uranium from the sample, oxygen, and water (Wronkiewicz et al., 1996). The sequence of alteration phases on the top of the sample surface within 3.5 years of reaction is shown in Figure 6-1.

After 5,000 years of deposit, the phase transformation from uranium-bearing radionuclides waste to Schoepite is completed throughout the package (Wronkiewicz and Buck, 2000). Uranophane precipitates at the expense of schoepite only at the top layer of the package (Windt et al., 2003). The dissolution equations of relevant uranium-bearing mineral: Schoepite, Soddyite, Na-boltwoodite, and Uranophane, as well as hydrated neptunium oxide and plutonium oxide are listed in Table 6-1.

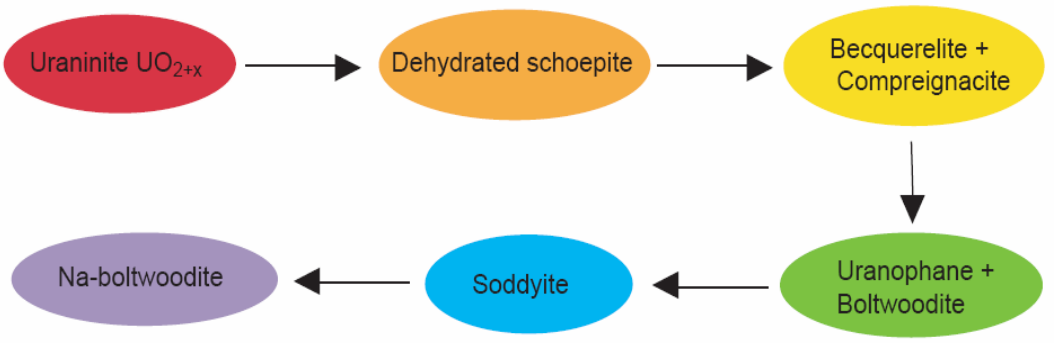

Figure 6-1. The Paragenetic Sequence of Alteration Phases on the Top of the Sample in the Experiment.

Table 6-1. Dissolution Equations of Principal Alteration Phases of Uranium, Neptunium, and Plutonium at 25ºC.

Phase Name	*Dissolution Equations*	*Log k*
Uranophane	$Ca(UO_2)_2(SiO_3OH)_2{\cdot}5H_2O + 6H^+ = Ca^{2+} + 2UO_2^{2+} + 2H_4SiO_4 + 5H_2O$ [a]	11.69
Schoepite	$UO_3H_2O + 2H^+ = UO_2^{2+} + 2H_2O$ [a]	4.84
Na-boltwoodite	$NaUO_2SiO_3OH{\cdot}1.5H_2O + 3H^+ = Na^+ + UO_2^{2+} + H_4SiO_4 + 1.5H_2O$ [a]	5.96
Soddyite	$(UO_2)_2SiO_4{\cdot}2H_2O + 4H^+ = 2UO_2^{2+} + H_4SiO_4 + 2H_2O$ [b]	6.03
PuO_2	$PuO_2 + 4H^+ = Pu^{4+} + 2H_2O$ [b]	-1.02
Np_2O_5	$Np_2O_5 + 2H^+ = 2NpO_2^+ + H_2O$ [a]	5.2

a DTN: SN0504T0502404.011
b DTN: MO0312SPATHDMIF.000

Based on the analyses in Table 6-1 and Figure 6-1, the equilibrium constant data indicate that Schoepite is the lease soluble of the other uranium-bearing minerals. Therefore, we consider the Schoepite as the solubility-controlling mineral of uranium, which has been verified by some researchers (Wronkiewicz and Buck, 2000; Davis and Curtis, 2003). The dissolution equations are implemented into PHREEQC to calculate the dissolution concentration of total uranium-bearing species. Results are used for the second step of simulation: aqueous speciation. With a range of different pH and f_{CO2} values, we may obtain different concentrations of dissolved uranium-bearing minerals. All the results will provide a base for the coupled geochemical and transport modeling.

6.3.3 Hydrated Neptunium Oxide Solubility

Laboratory experiments and observations of natural systems provide the basis for choosing the controlling phase of neptunium. For example, experiments in J-13 well water show $Np_2O_5 \cdot xH_2O$ is the controlling solid (Efurd et al., 1998) for the time scale of the experiments (250 days).

The solubility of neptunium decreases with an increase of pH value (Kaszuba and Runde, 1999). Equilibrium thermodynamics predicts NpO_2 as the predominant stable solid for most pH and Eh conditions, whereas in the absent of NpO_2, Np_2O_5, and $Np(OH)_4$ (amorphous) are the stable solids in groundwater at both oxidizing and reducing conditions in the YM groundwater system (Kaszuba and Runde, 1999). The dissolution equation of neptunium oxide is listed in Table 6-1.

6.3.4 Plutonium Solubility

Solubility data for the dissolution of plutonium dioxide (PuO_2) and tetrahydroxide ($Pu(OH)_4$) in laboratory and natural waters are compared with results of modeling calculations by Haschke and Bassett (2002). Their evaluation shows that the selection of $Pu(OH)_4$ as the solubility-controlling solid results in predicted steady-state plutonium concentrations that are not conservative and oxidation-state distributions that are inconsistent with observations. However, the observed co-existence of both crystalline and amorphous materials in plutonium solubility experiments by OCRWM (2003a) can be explained by the aging of precipitates. Therefore it appears that the solubility-controlling solids in those laboratory experiments are $Pu(OH)_4$, which "age towards $PuO_2 \cdot xH_2O$" (CRWMS M&O, 2001). The value of X could vary from 2 to 0. For X = 2, it is $Pu(OH)_4$, the amorphous end member. For X = 0, it is PuO_2, the crystalline end member. The crystalline phase has been formed within a laboratory time scale (less than one year), so it is reasonable to expect that over geological time, plutonium hydroxides will convert to PuO_2(c) (OCRWM, 2003a). Therefore, PuO_2 should be used as the solubility-controlling mineral for plutonium in the model.

In general, plutonium is approximately 3 orders of magnitude less soluble than neptunium and the pH value does not affect the solubility of plutonium as much as neptunium, which is 1 to 2 orders of magnitude from pH 6 to 8 (Efurd et al., 1998). The

dissolution equation of the selected plutonium solubility-controlling mineral PuO_2 is listed in Table 6-1.

6.4 TECHNICAL ISSUES IN SPECIATION EVALUATION

When percolating water continues flowing through the waste container, the alteration phases of radionuclides, especially those on the bottom of the rod or the RWP, would be further dissolved by water. Even though the solubility constants for the alteration phases are relatively low, the minerals on the bottom of container have no chance to re-precipitate inside. Therefore, the dissolved aqueous species would escape with the percolating water toward rock matrices and fractures beneath the disposal repository.

6.4.1 The Definition of Aqueous Speciation

The speciation refers to the form that one element is in aqueous complexes, redox species, free ions, colloidal, etc. After dissolving by infiltration water and mixing with pore water in the UZ, the radionuclide-bearing species will undergo some specific chemical reactions, including carbonate complexing and hydrolysis reactions in the aquifer under equilibrium status, depending on the available geochemical components of mixing water. The reactions result in that some of the species becoming dominant in the solution, whereas some of the species are consumed.

6.4.2 Uranium Aqueous Speciation

Wateq4f.dat in PHREEQC database files is one of the databases for running Uranium Solution & Speciation Model. This database is donated as qualified data. Only one valence state is used in this model, which is VI, based on several literatures (Davis and Curtis, 2003 (valid when feroxic water with D.O. > 30 μm); Windt et al., 2001). The master species of uranium is defined as UO_2^{2+}. In order to make the simulations most close to the UZ geochemical conditions, we select the chemical compositions of ten water samples from UZ#16. The location of wells is plotted in Figure 6-2. This pore water chemical component is used in all speciation simulations including neptunium and plutonium. These sampling data are derived from the YM database and Technical Report of OCRWM (2001). For detailed view, Tables 4-1 and 4-2 in Section 4 provide the data lists. By mixing the dissolution solution from RWP and UZ pore water sample, new species of uranium are generated.

6.4.3 Neptunium Aqueous Speciation

Based on the water chemical components and geological setting of UZ, hydrolysis and carbonate reactions of neptunium are considered in the Solution & Speciation Model. There is no built-in database file for neptunium reactions in PHREEQC code, so the formation of speciation reactions are taken example from Kaszuba et al.(1999) and Viswanathan et al. (1998) and written into input data file. The log K values for corresponding reactions are derived from related YM databases (Table 4-1). There are

two valence states studied, IV and V. The master species is defined as NpO_2^+ (V) based on the neptunium solid dissolution reaction (Table 6-1). By mixing the dissolution solution from RWP and UZ pore water sample, new species of neptunium are generated.

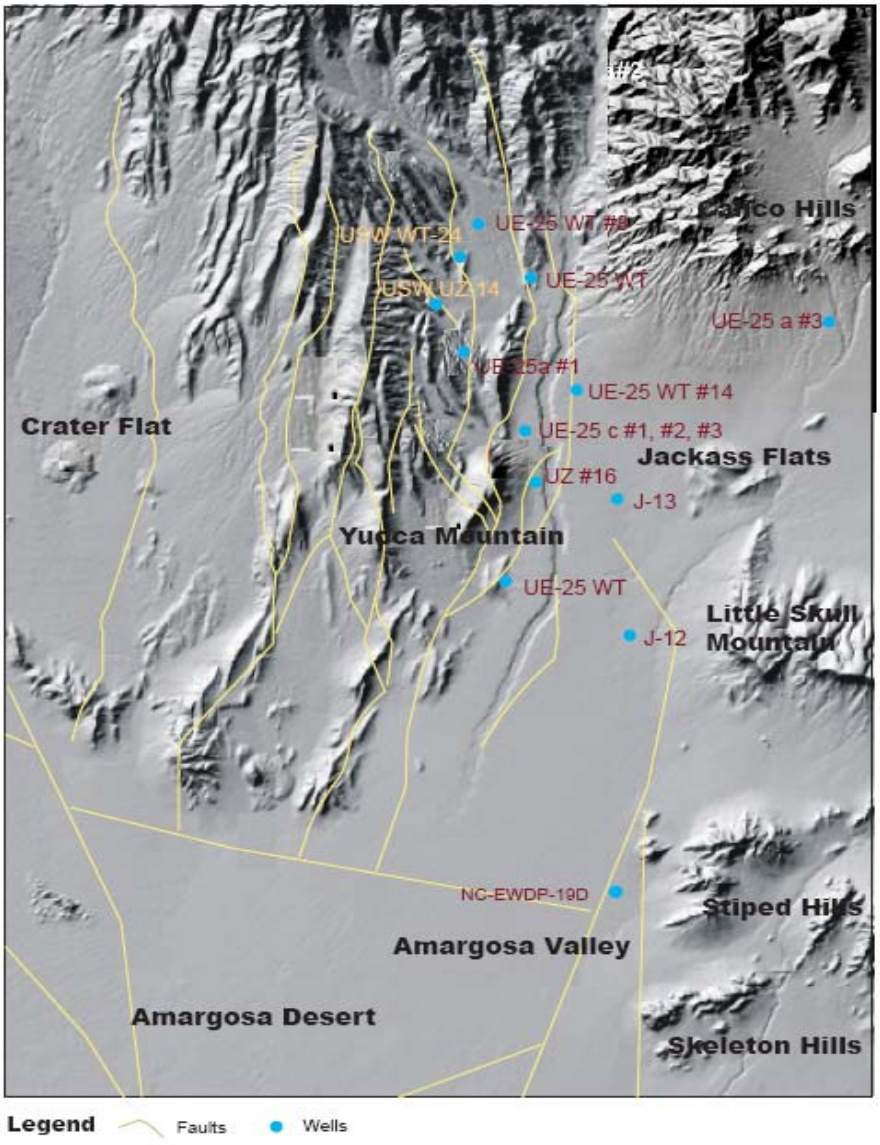

Figure 6-2. Major Geological Structures and Well Locations
(Background map is modified from BSC, 2003a).

6.4.4 Plutonium Aqueous Speciation

Hydrolysis, carbonate, as well as several sulfated reactions of plutonium are considered in the Solution & Speciation Model. There are four valence states studied in the model, which are III, IV, V, and VI. The master species is defined as Pu^{4+} (IV). At Nevada Test

Site, Pu has immigrated 1.3 km in 30 years in YM groundwater system by 7 nm to 1 μm colloids (Kersting et al.1999). According to Novikov et al. (2006), the surface complexation reactions and colloidal materials of Pu(IV) are more significant than its solution complexation behavior, however, the speciation of actinides or type of associated colloids is not well known (Novikov et al., 2006). Nevertheless, we focus on the solution complexation behavior here according to SIP-UNLV-045.

6.5 TREATMENT OF VARIATION AND UNCERTAINTY

Generally speaking, the solubility of an element in a repository is a variable, because the chemical conditions change over time (OCRWM, 2003a). Also, the uncertainty lies in the chemical conditions and the values of the parameters used in calculation. Uncertainty is associated with all steps in the model evaluation. For example, it can be associated with identification of a solubility-controlling solid and with the thermodynamic data used for the calculation (OCRWM, 2003a). Another factor affecting the uncertainty of model results is the use of average properties to describe geologic and hydrologic characteristics of the surrounding rock, chemical properties of the percolating, UZ pore water, and the groundwater.

There are four types of uncertainty, which are associated with the output of this report. They are uncertainties in the thermodynamic data supporting the PHREEQC calculations, uncertainties from variations in the chemistry of the water into which dissolution is occurring, composition of UZ water, as well as groundwater uncertainties in the temperature, and uncertainties from the accuracy of rate expression and kinetics reaction. For some elements, the identity of the solubility-controlling phase is also considered an additional source of uncertainty, especially neptunium and plutonium.

6.6 MODEL CONFIGURATION

Some important physical and chemical conditions for solubility and speciation evaluations are oxidation-reduction potential, pH, fCO_2, and temperature. This section explains how each parameter is accounted for in geochemical model calculations, whether they will be treated as an independent variable or as an uncertainty term, and how each parameter is varied.

6.6.1 Temperature

Solubility is calculated at 25°C. As shown in the next section, only the solubility of uranium is calculated with changing temperature from 25°C to 50°C. There is not enough thermodynamic data for other actinide elements in YM databases, no solubility simulation conducted by changing the temperature. Based on the result of uranium, using actinide solubility at 25°C would be conservative for temperatures higher than 25°C.

6.6.2 pH

The pH value has strong effect on actinide solubility, and so is selected as an independent variable in solubility calculations. Solubility calculations are carried out for different pH values. To cover both types of waste packages and possible extreme conditions, a pH range from 4.0 to 10.0 was chosen for solubility sub-model and varied in increments of 0.5 pH units. A pH range of 7.5 to 8.5 was chosen for UZ pore water as well as groundwater and varied in increments of 0.1 pH units for aqueous speciation sub-model.

6.6.3 CO_2 Fugacity

As discussed above, fCO_2 is another important independent variable in actinide solubility models because of the strong tendency for actinides to form complexes with CO_3^{2-}. The atmospheric value of CO_2 partial pressure is $10^{-3.5}$ bars. *Dissolved Concentration Limits of Radioactive Elements* (OCRWM, 2003a) gives the range of log f_{CO2} from -2.0 to -2.8 log bars. This is also the value used in *In-Package Chemistry for Waste Forms* (BSC 2001). Based on above technical reports, the representative fCO_2 value is between -2.2 to -3.1 and a mean value of –2.6 is chosen for further simulation needed. The fCO_2 range used for only actinide solubility calculations in this report is from $10^{-3.6}$ to $10^{-2.0}$ bars (same here) with an increment of 0.4 log units.

6.6.4 Oxidation Potential

The oxidation state is assumed to be controlled by the atmosphere (see Section 5). To achieve this condition, the value of fO_2 is set to 0.2 bars (OCRWM, 2003a).

6.7 URANIUM SOLUBILITY AND SPECIATION RESULTS

6.7.1 Solubility Results

When contacting with percolating water, these minerals would be dissolved based on their dissolution equations. After a long period of contact with solution in the waste package, all dissolution reactions could reach equilibrium and certain uranium minerals are dissolved. By changing over a range of pH values from 4.0 ~ 10.0, and partial pressure of CO_2 from -2.0 ~ -3.6 (BSC, 2005a) to cover both types of waste packages and possible extreme conditions, the amount of dissolved uranium changes (Figure 6-3).

Calculation results of uranium dissolution concentration based on solubility constant K_s are listed in Table 6-2. The concentration altered by CO_2 fugacity (partial pressure) and pH value is visualized in Figure 6-3. The increment for pH value is set as 0.5 pH units and log fCO_2 has an increment of 0.4 log units, as the same scenario for neptunium and plutonium. Among 65 calculations, 4 calculations are beyond valid ionic strength range that are marked as “ionic strength > 1”. Of those converged calculations that are listed in Table 6.2, the maximum concentration is 1.3×10^{-1} mol/L, which appears at pH = 9.5 / log fCO_2 = -2.4. The minimum concentration is 1.58×10^{-7} mol/L, which appears at pH

= 4 / log fCO_2 = -3.6. Based on the reversed "L" shape curves in Figure 6-3, several main points can be summarized. 1) The dissolution concentration is essentially constant for pH < 6, whereas increases rapidly for pH> 6.5. 2) With the same pH value, the higher the fCO_2 value, the higher the dissolution concentration. 3) Five curves represents different fCO_2 values are almost parallel between each other.

The dissolution concentration of uranium increases almost two orders of magnitude due to pH increase in a more realistic range of 7.5 to 8.5. By using SI to indicate uranium secondary mineral dissolution/precipitation processes, some observations are provided here. No matter how much pH increases, uranophane will not dissolve; where Na-boltwoodite has an essentially constant dissolution concentration of around 4.0×10^{-3} mol/L. When pH is higher than 8.2, soddyite begins to dissolve. At point of pH = 8, schoepite has its lowest concentration of 1.48×10^{-3} mol/L and then increases to 3.14×10^{-3} by pH = 8.5. Dissolution of Na-boltwoodite and schoepite contributes to the entire tendency of dissolution increase of uranium. When partial pressure of CO_2 increases with fixed pH = 8, soddyite precipitates much less where schoepite dissolves more. Also, the concentration of uranyl carbonate species increases because the increase of concentration of CO_3^{2-} that complex with UO_2^{2+}. These processes result in the increase of total concentration of uranium. The total dissolved uranium increases with pH increase, and the dissolution concentration of four minerals changes differently from each other (Figure 6-5).

A range of surrounding environmental temperatures (15~50 ºC) was used in the simulation to evaluate how the temperature could affect the dissolution simulation of uranium. The results indicate that the concentration of uranium in solution increases as temperature increases (Figure 6.6). When temperature is greater than 40 ºC, the concentration of dissolved uranium undergoes a significant increase.

Table 6-2. Calculated Uranium Dissolution concentration Controlled by Secondary Minerals (mol/L) (DID: R02YL.002).

pH/pCO2	-2	-2.4	-2.8	-3.2	-3.6
4	1.93E-06	5.30E-07	2.47E-07	1.78E-07	1.58E-07
4.5	1.97E-06	5.35E-07	2.47E-07	1.78E-07	1.58E-07
5	2.08E-06	5.55E-07	2.51E-07	1.79E-07	1.58E-07
5.5	2.45E-06	6.26E-07	2.67E-07	1.83E-07	1.59E-07
6	3.85E-06	8.82E-07	3.20E-07	1.97E-07	1.63E-07
6.5	1.05E-05	2.04E-06	5.46E-07	2.49E-07	1.78E-07
7	5.32E-05	9.18E-06	1.81E-06	5.02E-07	2.39E-07
7.5	4.05E-04	6.72E-05	1.14E-05	2.19E-06	5.72E-07
8	3.38E-03	6.06E-04	1.00E-04	1.68E-05	3.09E-06
8.5	2.23E-02	5.33E-03	9.96E-04	1.67E-04	2.75E-05
9	9.38E-02	3.20E-02	8.84E-03	1.85E-03	3.23E-04
9.5	ionic strength >1	1.30E-01	4.74E-02	1.55E-02	4.02E-03
10	ionic strength >1	ionic strength >1	ionic strength >1	9.29E-02	3.22E-02

Minimum red font; maximum blue font.

Output DID: R02YL.002
Notes: The output results are stored in Uranium Solubility \ Reduced Data \ files names: Uranium Solubility Reduced.txt.

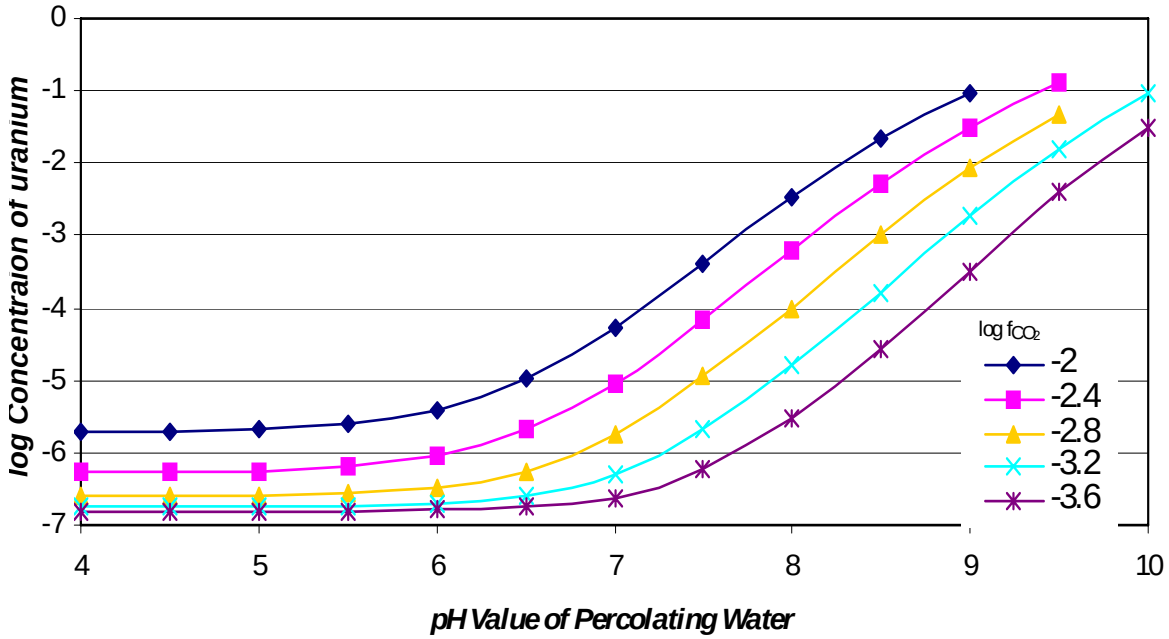

Output DID: R02YL.002
Notes: The output results are stored in Uranium Solubility \ Reduced Data \ files names: Uranium Solubility Reduced.txt. (X-column 1; Y-column 3)

Figure 6-3. Uranium Solubility Modeled as a Function of pH and fCO_2

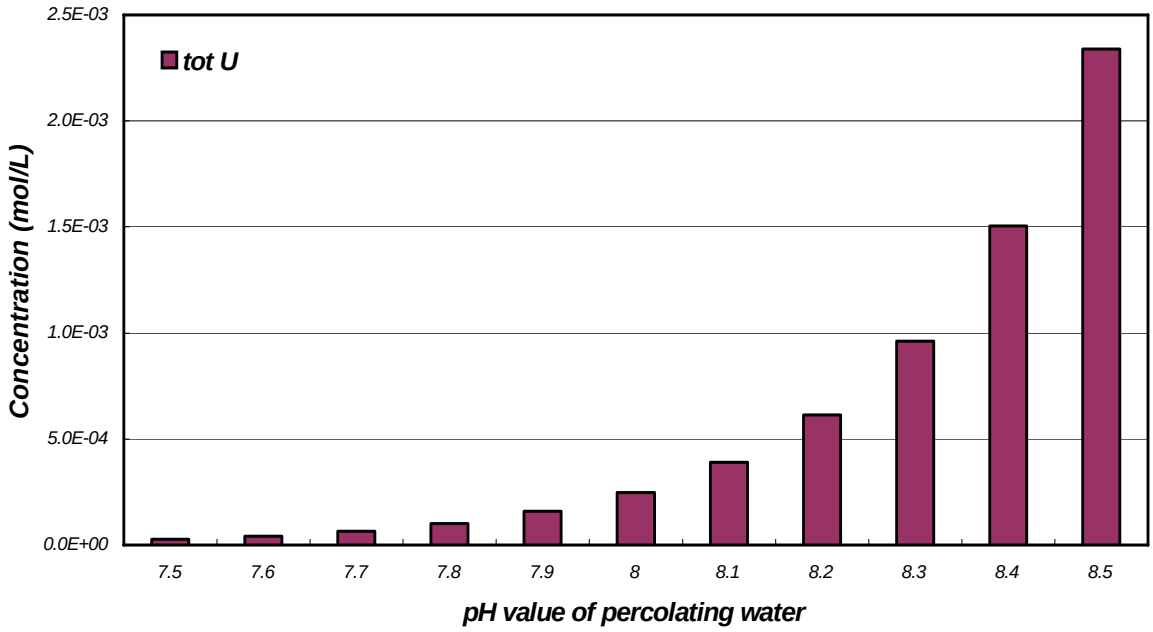

Output DID: R02YL.002
Notes: The output results are stored in Uranium Solubility \ Raw Data \ file names: USM dissolution pH.out, for example, USM dissolution 7.5.out.

Figure 6-4. Uranium Solubility Modeled by Percolating Water (pH = 7.5~8.5) in RWP

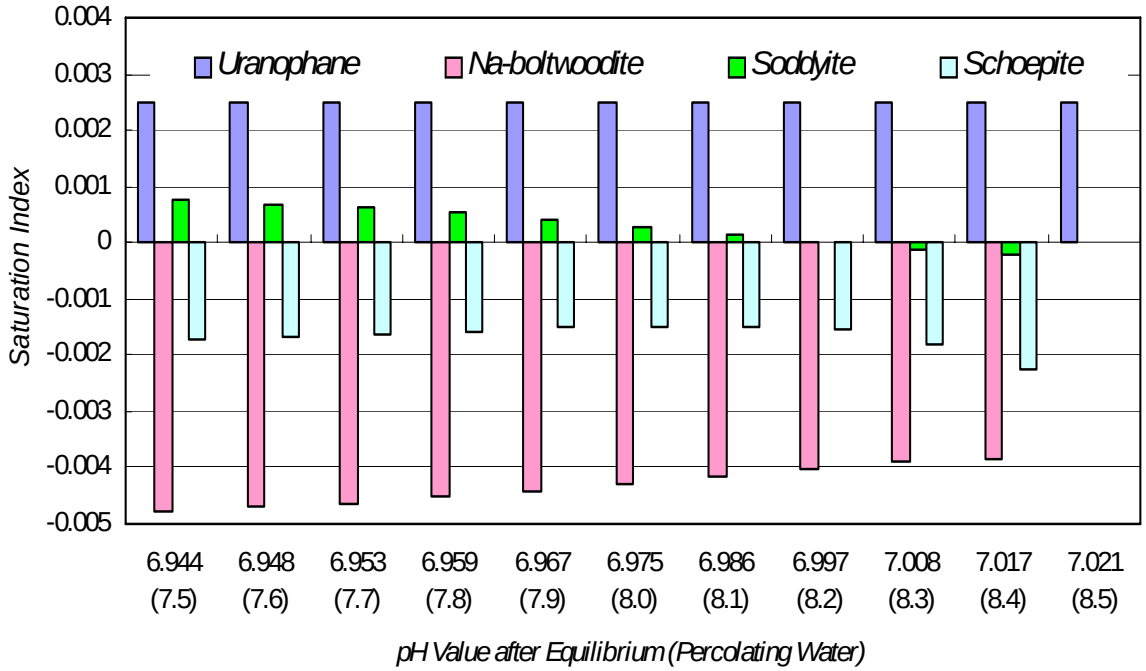

Output DID: R02YL.002
Notes: The output results are stored in Uranium Solubility \ Raw Data \ file names: USM dissolution pH.out, for example, USM dissolution 7.5.out.

Figure 6-5. Analyses of Uranium Secondary Minerals Solubility within RWP.

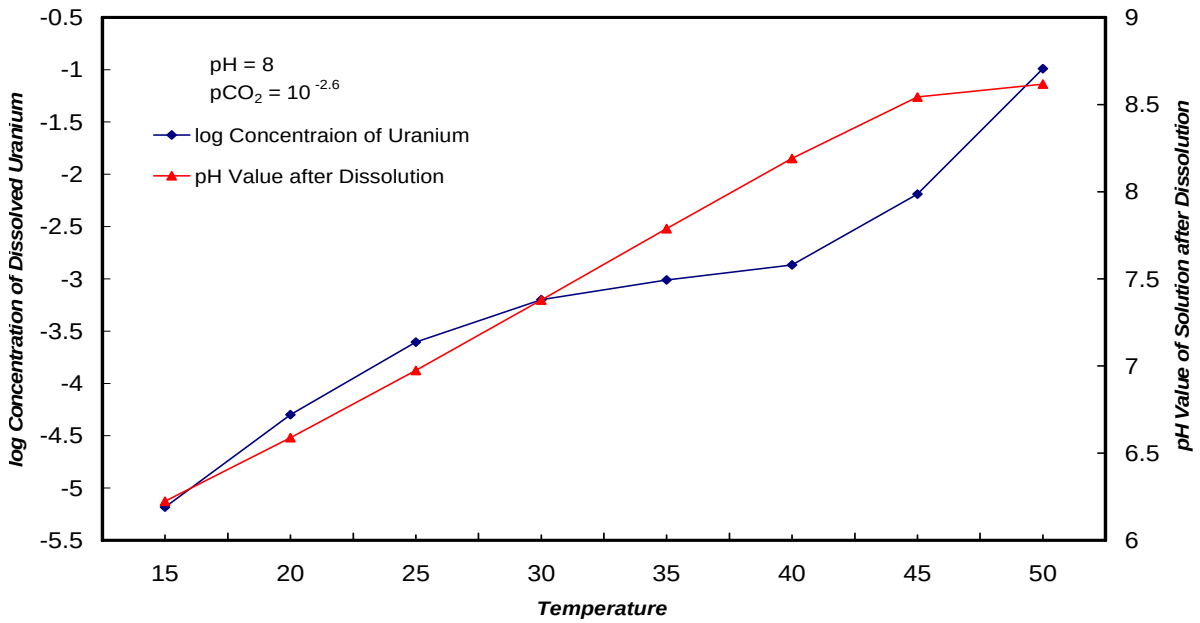

Output DID: R02YL.002
Notes: The output results are stored in Uranium Solubility \ Reduced Data \ file names: temperature.txt (X-column 1; Y-column 3, 4).

Figure 6-6. Uranium Dissolution concentration Changes with Increasing Temperature.

6.7.2 Speciation Results

The equilibrium solution with a certain amount of uranium species would escape from the RWP and migrate downward into the UZ. During this procedure, uranium aqueous speciation is calculated based on the geochemical composition of UZ pore water. The major ion concentrations are averaged from 10 samples of UZ pore water from different depth, 290 ~ 414 m (950 ~ 1400 feet) below ground surface. The pH value is over a range of 7.5~8.5 (OCRWM, 2001) and log fCO_2 is fixed at –2.6.

Uranium speciation results are plotted in Figure 6-7 for uranyl carbonate species and Figure 6-8 for uranyl hydroxide species. The concentration of dominating species does not change too much over one unit of pH, so the diagram is shown in column instead of straight line.

The concentration of uranyl carbonate species is several orders of magnitude higher than uranyl hydroxide species. In Figure 6-7, $UO_2CO_3^{2-}$ is the predominant species over other uranyl carbonate species within the pH range shown, and its concentration decreases whereas the concentration of $UO_2(CO_3)_3^{4-}$ slightly increase as pH increases. In Figure 6-8, $UO_2(OH)_3^-$ is the predominant species over other uranyl hydroxide species and its concentration remains constant over the pH range. The concentration of UO_2OH^+ is secondary in uranyl hydroxide species and decreases when pH increases.

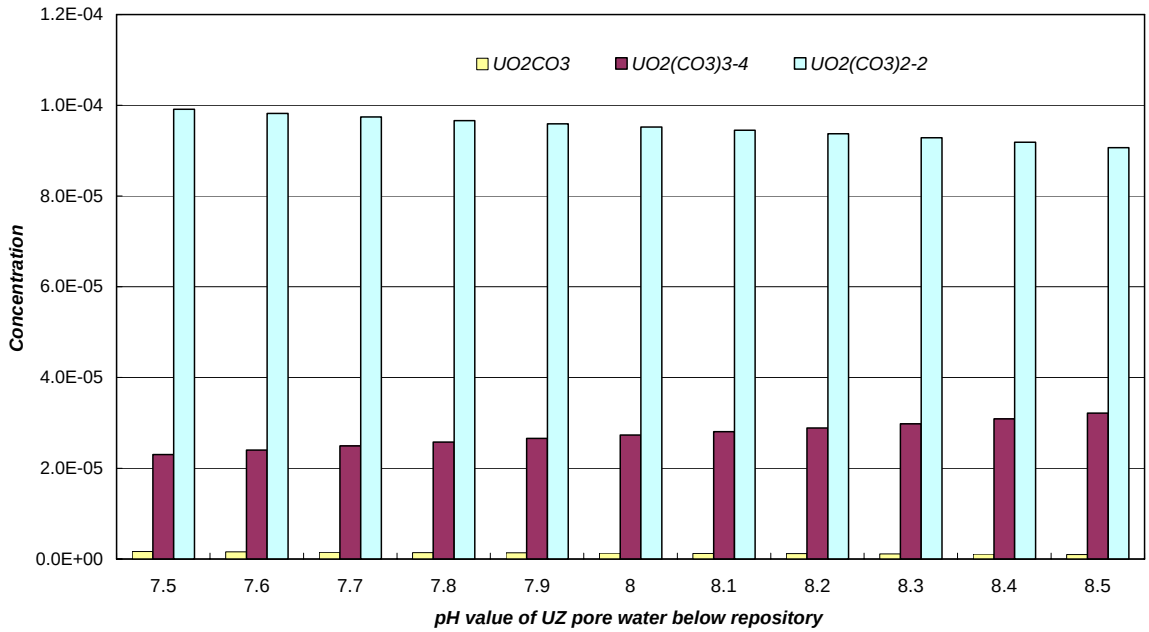

Output DID: R02YL.002
Notes: The output results are stored in Uranium Speciation \ Raw Data \ file names: "UASpH".out, for example, UAS7.5.out.

Figure 6-7. Uranium Aqueous Speciation of Uranyl Carbonate Species after Equilibrium with the UZ Pore Water.

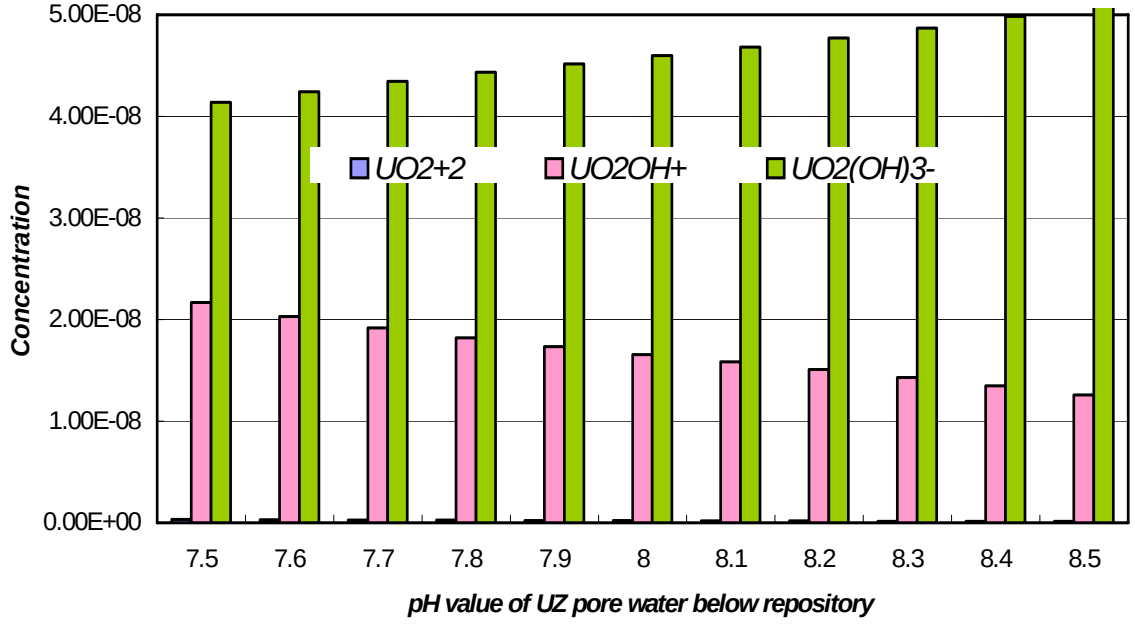

Output DID: R02YL.002
Notes: The output results are stored in Uranium Speciation \ Raw Data \ file names: "UASpH".out, for example, UAS7.5.out.

Figure 6-8. Uranium Aqueous Speciation of Uranyl Hydroxide Species after Equilibrium with the UZ Pore Water.

6.8 NEPTUNIUM SOLUBILITY AND SPECIATION RESULTS

6.8.1 Solubility Results

Among all constituents of spent nuclear fuel (SNF), neptunium is less than 0.1%. The solubility of neptunium is more complex than uranium. From several published literature sources (Kaszuba and Runde, 1999; Efurd et al., 1998; Nitsche et al., 1993), neptunium is two or three orders less soluble than uranium. Several pure neptunium phases have been identified in neptunium dissolution experiments, including Np_2O_5, $NaNpO_2CO_3 \cdot xH_2O$, and NpO_2. At the conditions relevant to the repository (oxidizing conditions and temperature from 25 to 90ºC), the precipitates in experiments are $Np_2O_5 \cdot xH_2O$ and $NaNpO_2CO_3 \cdot xH_2O$ (Efurd et al., 1998; Nitsche et al., 1993, p. 37).

Even though $NaNpO_2CO_3 \cdot xH_2O$ was observed in neptunium dissolution experiments using J-13 well water, a detailed analysis by Kaszuba and Runde (1999) found that $NaNpO_2CO_3 \cdot 3.5H_2O$ is stable only for the case when $[Na^+]$ is greater than 0.05 molar at neutral pH. Theoretical calculations using different thermodynamic databases (CRWMS, 2001) predict that the solubility controlling solid phase would be either a Np (IV) or Np (V) compound, depending on the redox state of the water. The solubility of solid phase with different oxidation states is quite different, with the Np (IV) phase having dissolution concentration several orders of magnitude less than that of Np (V) phase. Equilibrium thermodynamics predicts NpO_2 as the predominant stable solid for most pH and Eh conditions (CRWMS, 2001). In the absence of NpO_2, Np_2O_5 and $Np(OH)_4$ (amorphous) are the stable solids in waters at both oxidizing and reducing conditions in the YM groundwater system (Kaszuba and Runde, 1999).

Based on the X-ray diffraction data and by further analyzing the stability field for Np(V) solid phases (Np_2O_5, $NpO_2(OH)$, and $NaNpO_2CO_3 \cdot 3.5H_2O$), the report concludes that Np_2O_5 is the solubility controlling phase in J-13 well water under oxidizing conditions (CRWMS M&O, 2001). Also, the EQ3NR geochemical model conducted by OCRWM also selected Np_2O_5 to be a solubility controlling solid (OCRWM, 2003a). Consequently, we consider Np_2O_5 to be a solubility-controlling solid in this study. Calculation results of neptunium dissolution concentration based on solubility constant K_s are shown in Table 6-3.

In this case, there are 4 calculations beyond valid ionic strength ranges. The remaining 59 converged calculations listed in Table 6-3, with a maximum of 6.29×10^{-3} mol/L at pH = 9.5 / log f_{CO2} = -2.4 and a minimum of 4.07×10^{-6} mol/L at pH = 8.5 / log f_{CO2} = -3.6. For the log fCO_2 from –2, -2.4, -2.8, -3.2, to –3.6, the low points of dissolution concentration change from 7.5, 7.8, 8.0, 8.1, to 8.4 respectively. The concentration decreases slightly from pH 4 to 8, whereas it increases dramatically for pH above 8.0.

The tendency of neptunium dissolution concentration altered by f_{CO2} and pH appears in a "V" shape curves in Figure 6-9. In general, the concentration changes from high to low as pH changes from 4 to 8, and then back to high again as pH changes from 8 towards 10.

This is in line with neptunium dissolution experiment conducted as well as conclusion extrapolated by Efurd et al. (1998), which stated that neptunium average dissolution concentration decreased with increasing pH whereas increased with further increasing pH due to the formation of higher complexed anionic neptunium species in solution (Efurd et al., 1998). For a given pH value, the higher the fCO_2 value, the higher the concentration, which is identical to these changes of uranium. Calculated dissolution concentration curves with different fCO_2 values do not cross each other. As pH beyond 8, the concentration increases faster than the lower pH values.

From the enlarged dissolution concentration curve of Np_2O_5 under pH 7.5 to 8.5 (fCO_2 = 2.6), which represents percolating water, in Figure 6-10, the concentration has the lowest point of 1.21×10^{-5} mol/L for pH = 7.8 / log fCO_2 = 2.6.

Table 6-3. Calculated Neptunium Dissolution Concentration Controlled by Np_2O_5 (mol/L).

pH/ lgf_{CO2}	-2	-2.4	-2.8	-3.2	-3.6
4	2.75E-04	1.95E-04	1.55E-04	1.36E-04	1.28E-04
4.5	2.12E-04	1.26E-04	7.96E-05	5.74E-05	4.78E-05
5	1.90E-04	1.04E-04	5.65E-05	3.36E-05	2.38E-05
5.5	1.73E-04	9.40E-05	4.86E-05	2.62E-05	1.70E-05
6	1.43E-04	8.29E-05	4.39E-05	2.34E-05	1.49E-05
6.5	9.07E-05	6.18E-05	3.69E-05	2.10E-05	1.38E-05
7	4.22E-05	3.41E-05	2.49E-05	1.67E-05	1.20E-05
7.5	2.44E-05	1.72E-05	1.33E-05	1.05E-05	8.62E-06
8	3.94E-05	1.80E-05	9.67E-06	6.29E-06	4.84E-06
8.5	1.26E-04	4.64E-05	1.87E-05	8.18E-06	4.07E-06
9	1.09E-03	2.07E-04	6.23E-05	2.28E-05	9.07E-06
9.5	Ionic strength>1	6.29E-03	6.85E-04	1.13E-04	3.20E-05
10	ionic strength>1	ionic strength>1	ionic strength>1	5.48E-03	5.38E-04

Minimum red font; maximum blue font.

Output DID: R02YL.002
Notes: The output results are stored in Neptunium Solubility \ Reduced Data \ file names: Neptunium Solubility Reduced.txt.

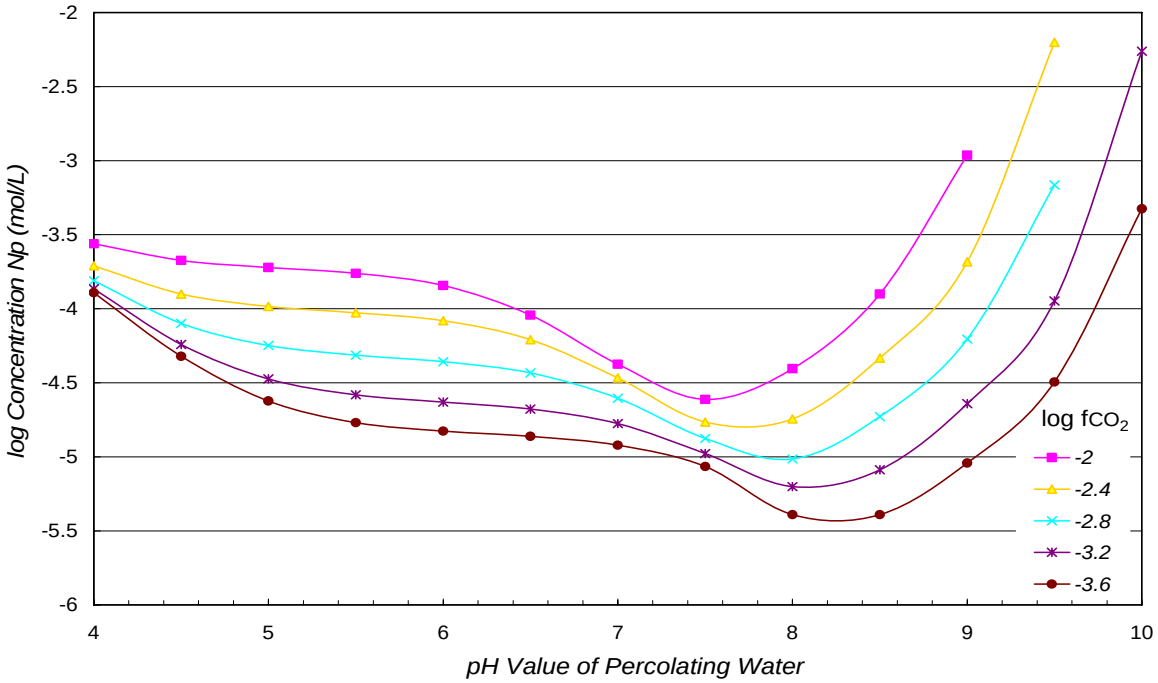

Output DID: R02YL.002
Notes: The output results are stored in Neptunium Solubility \ Reduced Data \ file names: Neptunium Solubility Reduced.txt. (X-column 1; Y-column 3)

Figure 6-9. Neptunium Solubility Modeled as a Function of pH and pCO_2.

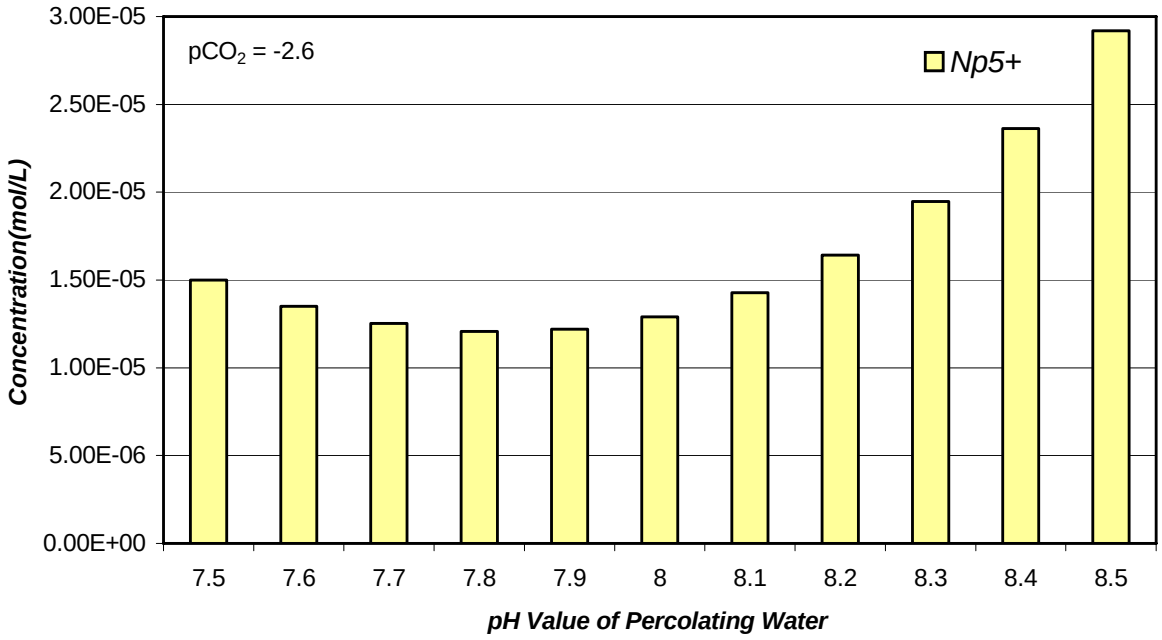

Output DID: R02YL.002
Notes: The output results are stored in Neptunium Solubility \ Reduced Data \ file names: 7.5 to 8.5 and -2.6.out (X-column 1; Y-column 2)

Figure 6-10. Neptunium Solubility Modeled by Percolating Water (pH = 7.5~8.5) in RWP.

6.8.2 Speciation Results

Neptunium aqueous speciation is shown in Figure 6-11 using semi-log axis over a pH range from 7.5 to 8.5 of UZ pore water, which are the identical samples used in last simulation. The predominant species is $NpO_2CO_3^-$ and its concentration slightly increases as pH increasing. This is caused by more and more available CO_3^{2-} ion as pH value increases. NpO_2^+ is the secondary dominant species whose concentration decreases with pH increase since Np (V) is consumed to form $NpO_2CO_3^-$.

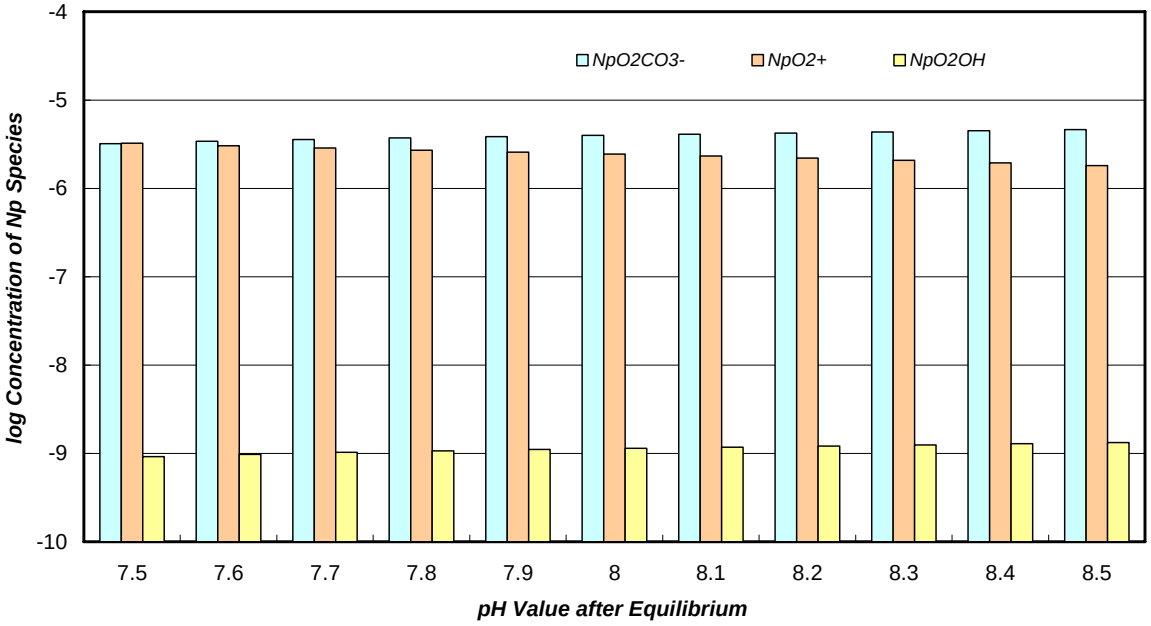

Output DID: R02YL.002
Notes: The output results are stored in Neptunium Speciation \ Reduced Data folder; file name: "pH".out, for example, 7.5.out. (X-column 1; Y-column 2, 3, 4)

Figure 6-11. Aqueous Speciation of Neptunium Species in the UZ.

6.9 PLUTONIUM SOLUBILITY AND SPECIATION

6.9.1 Solubility Results

In the past, numerous studies dealt with plutonium solubility (Nitsche et al., 1993; Rard, 1997; Kaplan et al., 2001), however, many uncertainties in understanding stability fields of plutonium solids remain. The geochemical model of solubility of plutonium minerals, using the YM database (DTN: MO0312SPATHDMIF.000), treats PuO_2 as the solubility-controlling solid, like most of the plutonium solubility studies, which is only valid for RWP. Some other studies use $PuO_2 \cdot 2H_2O$ (amorphous), which also could be written as $Pu(OH)_4$ or $PuO_2 \cdot xH_2O$. They are also denoted as hydroxide and aged, which means, "aged for several months near room temperature" (Lemire, 2001) and it actually means

more crystalline, less surface area per unit volume. Based on the observation of laboratory experiments conducted by Nitsche et al. (1993) using YM J-13 groundwater, the results of solid phase are the combination of crystalline and amorphous materials, which is consistent with the observed powder pattern. OCRWM (2003) concluded that the observed coexistence of both crystalline and amorphous materials in plutonium dissolution experiments could be explained with the aging of precipitates. The crystalline phase has been formed within the laboratory experiment time scale, so it is reasonable to assume that over some geological time, plutonium hydroxides will convert to PuO_2 (crystalline). Based on these analyses, PuO_2 could be used as the solubility-controlling mineral for plutonium in the waste package.
The dissolution equation of PuO_2 (K_{sp} is between -1 and -2) is listed in Table 6-1. The composition of selected initial percolating water is listed in Table 4-3. Similarly, the dissolution concentration calculations will be conducted over a range of conditions that are expected to include the actual conditions.

By similar procedures, the solubility simulation of plutonium has 4 calculations beyond valid ionic strength range listed in Table 6-4. Alteration of the plutonium dissolution concentration by different CO_2 fugacity and pH value is plotted in Figure 6-12 with a maximum of 2.35×10^{-9} mol/L at pH = 9.5 / log f_{CO2} = 2.4 and a minimum of 5.83×10^{-10} mol/L at pH = 10 / log fCO_2 = -3.6. Five curves in Figure 6-12 are overlapped together, which is different from that of uranium and neptunium.

Overall, the dissolution concentration of plutonium does not change much over both the pH values and CO_2 fugacity range. Also, plutonium is 6-7 orders of magnitude less soluble than uranium and 4-5 orders less than neptunium caused by chemical properties of plutonium element, which has been verified by some published literatures (Rard, 2000; Kaplan et al., 2001; CRWMS M&O, 2001; OCRWM, 2003b).

The dissolution concentration curves of uranium is a monotonic increasing function with exponential increasing instead of linear, whereas the neptunium are close to a serial of conic curves with the low points. Because the dissolved concentration would affect the aqueous species distribution as well as concentration, it is better to apprehend the more soluble one and give more concern in the next step. The overall dissolution concentration of neptunium centralizes from 10^{-4} to 10^{-5}, whereas uranium has a wide range from 10^{-1} to 10^{-7}, which looks difficult to determine. In the speciation simulation, however, a 7.5~8.5 pH range (OCRWM, 2001) with a fixed f_{CO2} = -2.6 is set to represent more realistic situ condition. Over this pH range and f_{CO2} value, the dissolution concentration of uranium is obviously higher than neptunium. For plutonium, it has a relative small dissolution concentration as a whole compared to the other two elements and less impact caused by CO_2 fugacity and pH values, which makes an easier approach to its speciation simulation.

Table 6-4. Calculated Plutonium Solubility Controlled by PuO_2 (mol/L)

pH/pCO_2	-2	-2.4	-2.8	-3.2	-3.6
4	1.21E-09	1.21E-09	1.21E-09	1.21E-09	1.21E-09
4.5	6.73E-10	6.73E-10	6.73E-10	6.73E-10	6.73E-10
5	6.12E-10	6.12E-10	6.12E-10	6.12E-10	6.12E-10
5.5	6.03E-10	6.03E-10	6.03E-10	6.03E-10	6.03E-10
6	6.01E-10	6.01E-10	6.01E-10	6.01E-10	6.01E-10
6.5	6.01E-10	6.01E-10	6.01E-10	6.01E-10	6.01E-10
7	6.01E-10	6.01E-10	6.01E-10	6.01E-10	6.01E-10
7.5	6.00E-10	6.01E-10	6.01E-10	6.01E-10	6.01E-10
8	5.99E-10	6.00E-10	6.01E-10	6.01E-10	6.01E-10
8.5	5.96E-10	6.00E-10	6.01E-10	6.01E-10	6.01E-10
9	8.34E-10	5.95E-10	5.98E-10	6.00E-10	6.00E-10
9.5	ionic strength>1	2.35E-09	5.97E-10	5.96E-10	5.99E-10
10	ionic strength>1	ionic strength>1	ionic strength>1	6.74E-10	5.83E-10

Minimum red font; Maximum blue font.

Output DID: R02YL.002
Notes: The output results are stored in Plutonium Solubility \ Reduced Data folder; files name: Plutonium Solubility Reduced.txt.

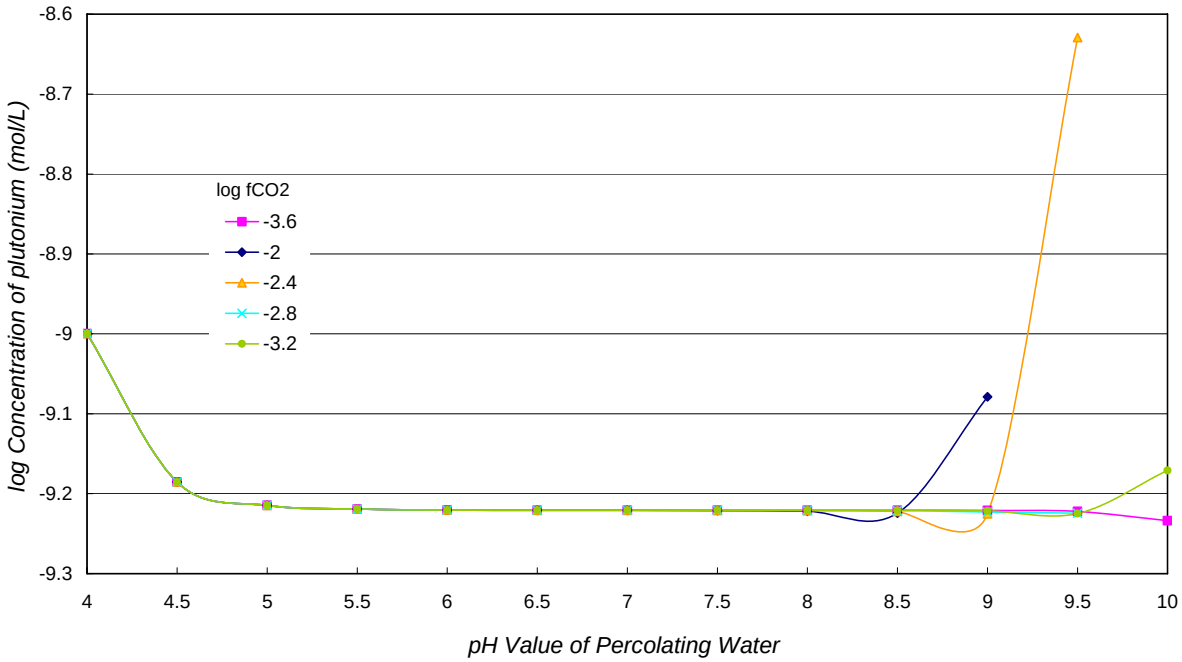

Output DID: R02YL.002
Notes: The output results are stored in Plutonium Solubility \ Reduced Data folder; files name: Plutonium Solubility Reduced.txt. (X-column 1; Y-column 3)

Figure 6-12. Plutonium Solubility Modeled as a Function of pH and pCO_2.

6.9.2 Speciation Results

Figure 6-13 shows the plutonium aqueous speciation diagram, which is identical to the samples used in uranium simulation. The obviously predominant species over pH of 7.5 ~ 8.5 is $Pu(OH)_4$ (aq). $Pu(OH)_3^+$ is the secondary dominant species and its concentration decreases slightly as pH is increased. The concentration of $Pu(CO_3)_2^-$ and $PuCO_3^+$ generates a small peak when pH is around 7.6 with the maximum value of 2.44×10^{-16}, 3.01×10^{-16} mol/L. When pH equals 8.5, the minimum concentration of $Pu(CO_3)_2^-$ and $PuCO_3^+$ is 4.64×10^{-17} and 2.47×10^{-17} mol/L, respectively. The concentration of $PuO_2CO_3^-$ has a low point of 9.9×10^{-18} for pH equals to 8.2, whereas a high point of 2×10^{-17} for pH equals to 7.5. The concentration of PuO_2^+ decreases one-third from pH =7.5 to 7.6 and then remains 5.1×10^{-18} mol/L for the rest of the calculations.

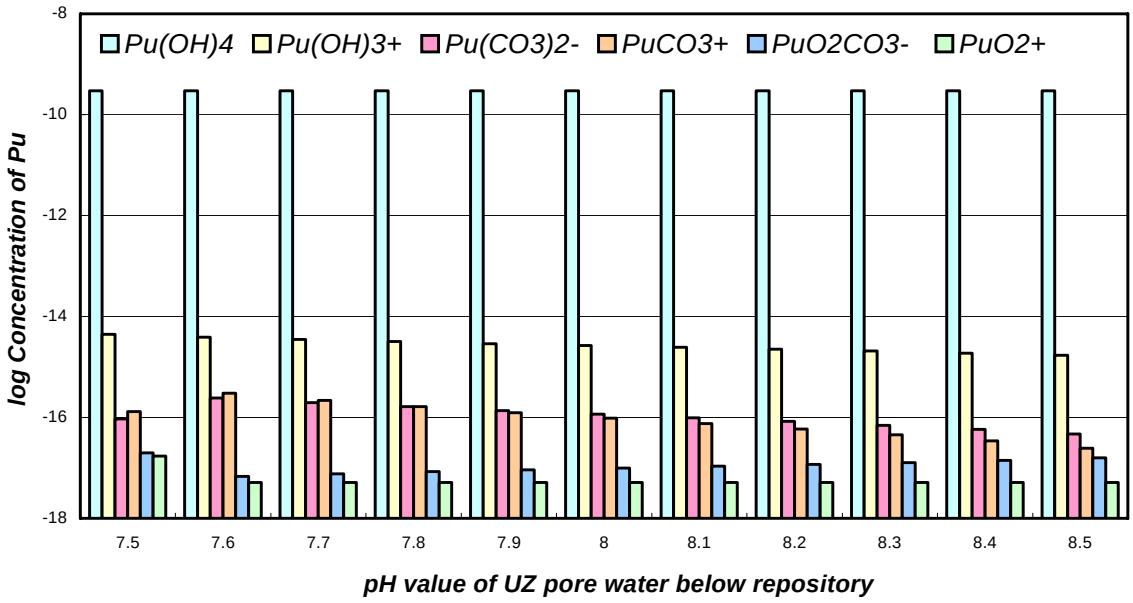

Output DID: R02YL.002
Notes: The output results are stored in Plutonium Speciation \ Reduced Data folder; file name: "pH".out, for example, 7.5.out. (X-column 1; Y-column 2, 3, 4, 5, 6, 7)

Figure 6-13. Plutonium Aqueous Speciation after Equilibrium with UZ Pore Water.

6.10 MODEL VALIDATION

6.10.1 Validation Criteria

The simulation model PHREEQC has two functions in this study. One is to calculate the solid solubility (dissolution concentration) after equilibrium based on the input dissolution reaction as well as thermodynamic data (log Ks). Another is to calculate the

aqueous speciation based on the input chemical reactions as well as thermodynamic data (log K). In its initial condition use, the dissolution concentration comes from the last step. This study followed the accepted method used in the conceptual model of Mitcheltree (Mitcheltree, 2006), and relies on the validation results provided by this study. The validation was done under the published report (DOC: 20061002.0009). The source code of PHREEQC was not altered during the whole application. As pointed out in Section 6.3, the solubility evaluation involves several technical aspects including: (1) thermodynamic database and a modeling tool; (2) environmental conditions; (3) construction of the conceptual model; and (4) the calculation of dissolution concentration limits using a geochemical modeling tool based on the conceptual model. Because all thermodynamic data used in this report and the PHREEQC code are controlled products (from YM database) and this report uses them within their valid ranges. Aspects (1) and (4) are exempted from model validation. Aspect (2) is the inputs to this report; thus, no model validation is necessary. Therefore, model validation discussed in this report focuses on Aspect (3): whether the conceptual model is appropriate (OCRWM, 2003).

The conceptual model as the input files to PHREEQC includes the following components: (1) percolating water penetrates into RWP and dissolves some radionuclide-bearing minerals. The dissolved minerals form a series of complex alteration phases or secondary minerals, then undergo re-precipitation and re-dissolution throughout the canisters; (2) some of the phases dissolved into solution finally leave the waste packages, and then enter the UZ; (3) traveling through UZ, the dissolved species lead to a series of chemical reactions, such as hydrolysis reaction, reaction with carbonate ligands over a range of pH value, and then the radionuclides get into SZ groundwater, contaminate the Amargosa desert groundwater water. These components of the conceptual model as well as assumptions are appropriate and all are good enough for the purpose of this use.

The selection of solubility-controlling solids, as documented in individual subsections of Sections 6.7 and 6.8, was based on literature prepared for DOE when they are available and conclusive (OCRWM, 2003a; BSC, 2004a; BSC, 2005). The literature is very comprehensive and includes both laboratory and field observations.

In the solubility simulations, we define solubility controlling solid as Phases and input dissolution reactions for each solid with reliable solubility product constant (K_{sp}) from the YM database. Based on the assumption that there is sufficient time for the dissolution reaction to reach equilibrium in RWP, the "Equilibrium Phases" keyword of PHREEQC was set in the solubility simulation to indicate equilibrium and obtain the dissolution concentration of phases under equilibrium status. In the aqueous speciation simulations, we follow the standard format (Ex.1) given by the PHREEQC instruction manual (Parkhurst, and Appelo, 1999) to prepare the input files. Especially, the PHREEQC database has uranium thermodynamic data available, which has been qualified, so we use this database directly without any additional reactions as well as log K values. For the other two elements, major hydrolysis and carbonate complexation reactions are entered in the input files with thermodynamic data selecting from YM database (Table 4.1).

6.10.2 Testing and Comparison

The solubility results are compared to the results from a DOE Technical Report: Dissolved concentration limits of radioactive elements (OCRWM, 2003). They all fall in the same range.

Aqueous speciation diagrams of neptunium and uranium from the paper of Viswanathana et al. (1998) and Davis & Curtis (2003) are selected for contrast comparison. The assumption is that there will be a long enough time (from repository to water table) for the speciation reactions to reach equilibrium.

The testing result below (Figure 6-14) shows the neptunium hydroxides and carbonate speciation reactions. For testing purpose, the thermodynamic data (log k) input to PHREEQC is derived from Kaszuba and Runde (1999). Assigned TOT CO_2 is 2.3×10^{-3} mol/L and TOT Np is 1×10^{-5} mol/L. The results are most consistent with these by Viswanathana et al. (1998) in Figure 6-15. For the actual simulations, all thermodynamic data are available and derived from the YM database.

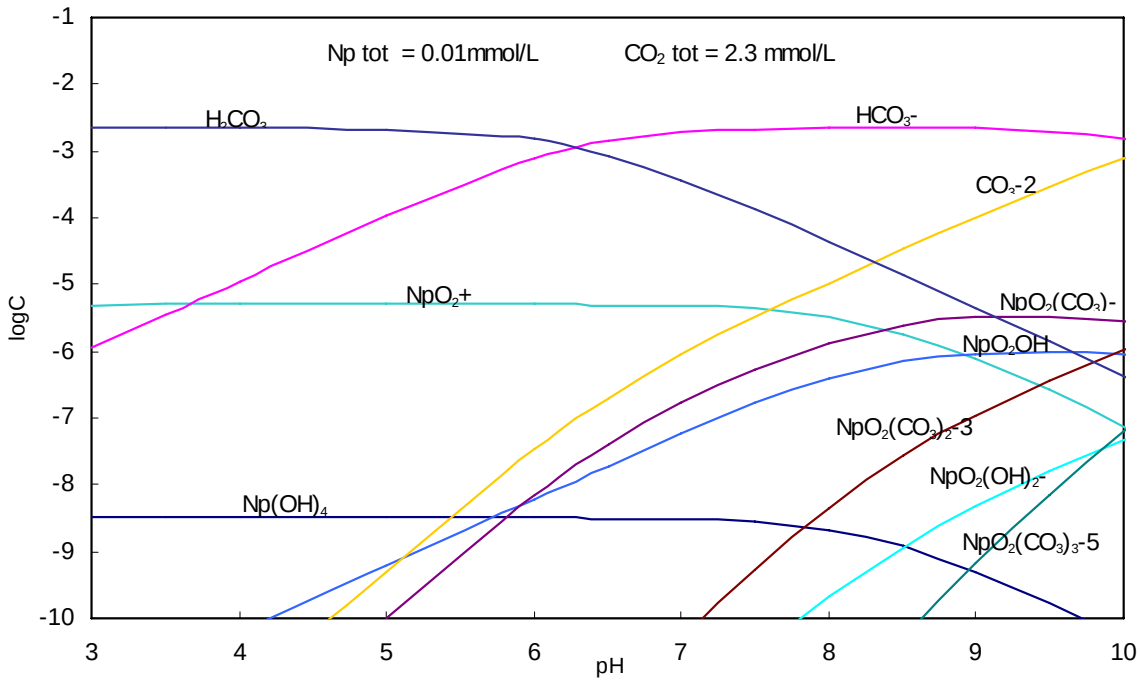

Figure 6-14. Aqueous Speciation Diagram of Neptunium at 25 °C
(Source: UCCSN-UNLV-087, v.3: UQ Data, use for information only).

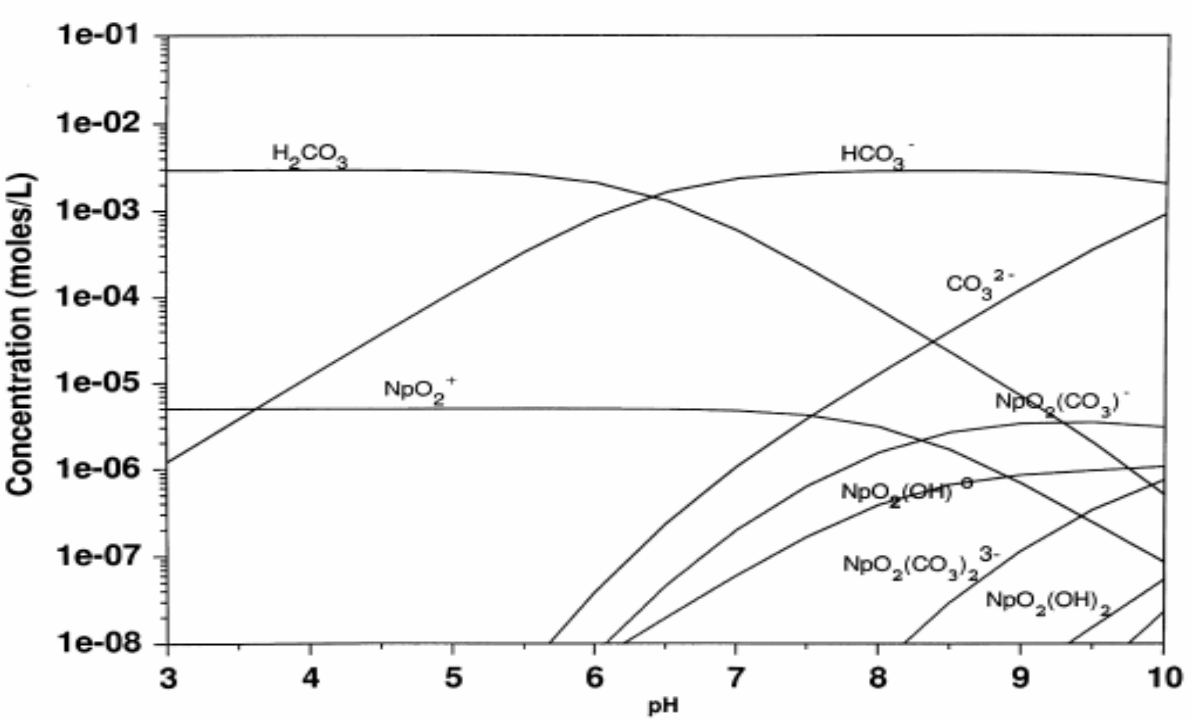

Figure 6-15. Aqueous Speciation Diagram of Neptunium in J-13 Water with a Dissolution Concentration of 1×10^{-5} mol/L (from Viswanathana et al., 1998) (UQ Data, use for information only).

From Efurd et al. (1999), the results of neptunium dissolution experiments show NpO_2^+, $NpO_2(OH)$, and $NpO_2CO_3^-$ (at pH 7-10) as the predominant species in the solution. Based on the testing run above, the predominating species is NpO_2^+ for pH lower than 8. The higher the pH value, the more the species appear, especially $NpO_2(CO_3)^-$ and $NpO_2(OH)$ as predominant species for pH is higher than 8.3, similar to those documented experiments by Efurd et al. (1998) and Kaszuba and Runde (1999). The concentration of $Np(OH)_4$ is minor and almost constant from pH 3 to 8.

Another example shows the concentration of hydrolysis and carbonate species of uranium verses pH values (Figure 6-16). Assigned TOT CO_2 is 5×10^{-2} mol/L and TOT U is 1×10^{-5} mol/L. The thermodynamic data, as inputs to PHREEQC, are obtained from Davis and Curtis (2003) (Figure 6-17).

The shape of the curves and values are consistent with the results of Davis and Curtis (2003). The predominant species between pH 6-8 is $UO_2(CO_3)_2^{2-}$, followed by $UO_2(CO_3)_3^{4-}$. The concentration of UO_2CO_3 and $(UO_2)_2CO_3(OH)_3^-$ decreases rapidly with the increase of pH value from 6 to 7.7.

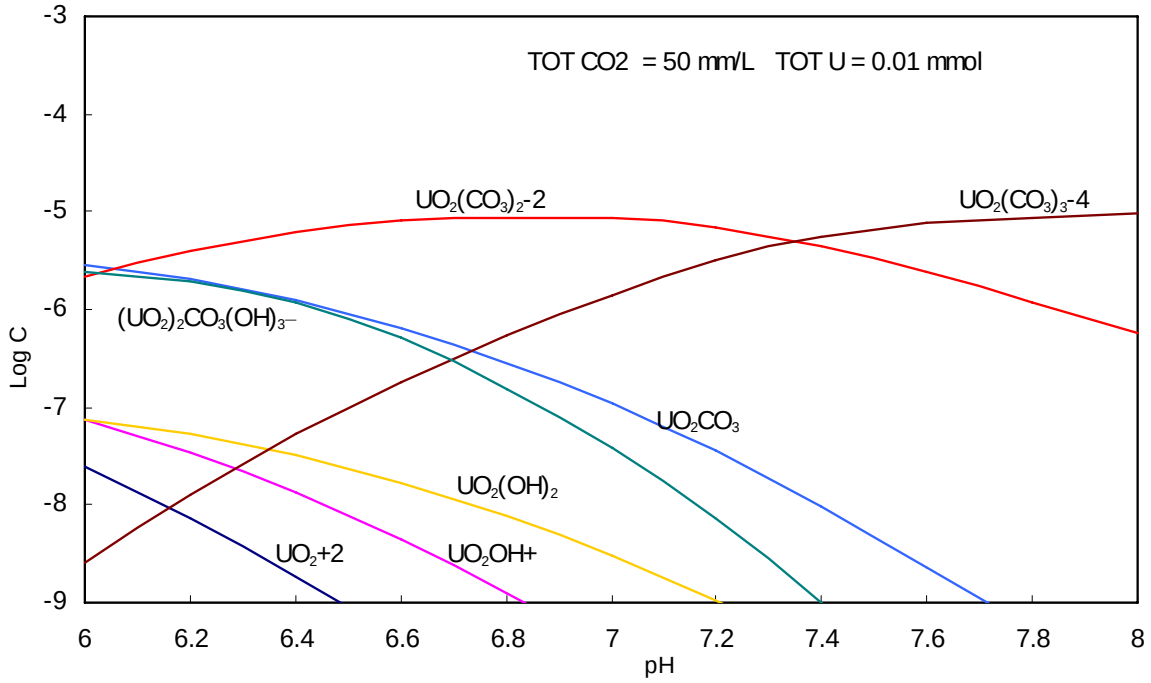

Figure 6-16. Aqueous Speciation Diagram of Uranium at 25 °C
(Source: UCCSN-UNLV-087, v.3: UQ Data, use for information only).

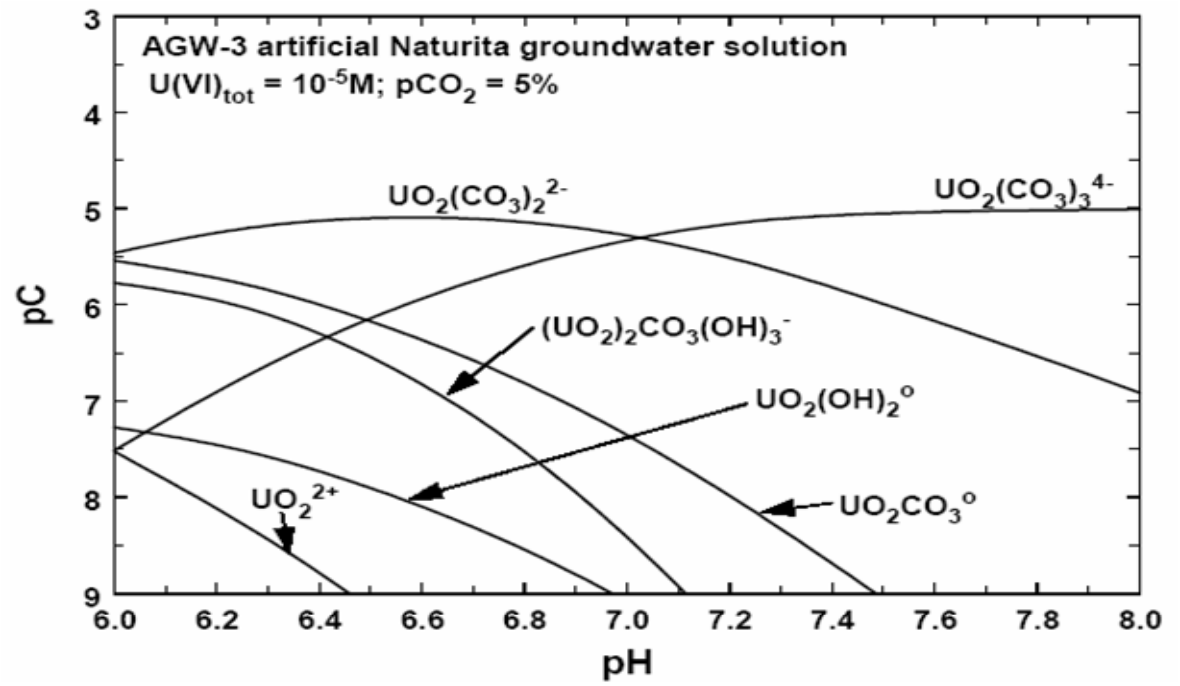

Figure 6-17. Aqueous Speciation of Uranium as a Function of pH in an AGW-3 Artificial Groundwater Solution Equilibrium with a Partial Pressure of CO_2 of $10^{-1.3}$ (Davis and Curtis, 2003) (UQ Data, use for information only).

7. CONCLUSIONS

7.1 MODEL OUTPUT

Three sub-model outputs are summarized in Table 7-1. The output for uranium, neptunium, and plutonium are in the form of Tables in Sections 6.6, 6.7, and 6.8. They are not repeated in this section.

Table 7-1. Summary of Three Sub-models

Element	Solubility	Speciation
U	See table 6-2	See figure 6-7, 6-8
Np	See table 6-3	See figure 6-11
Pu	See table 6-4	See figure 6-13

7.2 OUTPUT UNCERTAINTY

Uncertainties from various sources have been addressed in this report. The solubility sub-model has three groups of uncertainties. They consist of uncertainty in the selection of the solubility-controlling phase, uncertainty in log K_s of solubility controlling phase, and the uncertainty associated with temperature and pH variations. The speciation sub-model is subject to three uncertainties: Firstly, the pH range of 7.5-8.5 is assigned to the UZ pore water based on the average of water samples from UZ #16. Secondly, they have the uncertainty of the thermodynamic data (log K) from YM Database (see Table 4-1). Thirdly, the uncertainty of the results came from solubility sub-model.

7.3 RESTRICTIONS

As discussed in Section 6.3, the solubility, speciation, and transport models developed in this model report are valid for broad ranges of water composition, as listed in Table 7-3. They may be applied both inside and outside waste packages, UZ, as well as SZ. However, as stated in Section 6.3.6, the solubility sub-model is subject to three restrictions: Firstly, they are restricted to ionic strength not higher than 1 molal because the equations are used in model calculations. Secondly, because some calculations did not converge or give an ionic strength higher than 1 molal, the ranges of the tables may be narrowed from those given in Tables 6-1, 6-2, and 6-3. Within those tables, the value "ionic strength" was used to indicate that no dissolution concentration was given for those ranges of conditions. Thirdly, for any conditions outside the 4.0-11.0 pH range, the –2.0 to –3.6 fCO_2 range, the inventory concentrations calculated according to the dissolution rate of waste forms, infiltrating water volume, and radionuclide inventory should be used (OCRWM, 2003a).

Table 7-2. Summary of Uncertainty for Models

	I	II	III
Solubility	Solubility controlling phases	Log K_s	pH range, fugacity of CO_2 , and temperature
Speciation	pH range	Log K	Dissolved concentration
Transport	Rate expressions & Kinetic reactions	Transport parameters	Flow velocity

Table 7-3. Valid Range of the Solubility Models Reported in This Report

Variable	**Value or Range**
pH	-4 to -10
log fCO2	-3.6 to –2.0 bars
Temperature	25 ^{o}C
Ionic Strength	Less than 1 molal

8. INPUTS AND REFERENCES

8.1 DOCUMENTS CITED

Atkins, P.W., 1994. Physical chemistry, 5th *Ed*: New York W.H. Freeman and Company, New York, TIC: 246986.

Bechtel SAIC Company, 2004a, Site-scale saturated zone transport, November 2004: *Prepared for* U.S. Department of Energy, MDL-NBS-HS-000010 REV 02, 366 p.

Bechtel SAIC Company, 2003a, Saturated Zone Flow and Transport, Revision 2, September 2003: *Prepared for* U.S. Department of Energy, 402 p.

Bechtel SAIC Company, 2003b, Geochemical and isotopic constraints on groundwater flow directions and magnitudes, mixing, and recharge at Yucca Mountain, July 2003: *Prepared for* U.S. Department of Energy, ANL-NBS-HS-000021 REV 01, 505 p.

Bethke, C.M. and Brady, P.V., 2000, How the K_d approach undermines groundwater cleanup: Ground Water, v. 38, p. 435-443.

Canori, G.F. and Leitner, M.M. 2003, Project Requirements Document, TER-MGR-MD-000001 REV 01: Bechtel SAIC Company, Las Vegas, Nevada, ACC: DOC.20030404.0003.

CRWMS M&O, 2001, Pure phase solubility limits: ANL-EBS-MD-000017 REV 00 ICN 01, *Prepared for* U.S. Department of Energy, Las Vegas, Nevada, 230 p.

CRWMS M&O, 2000a, Saturated zone flow and transport process model report, August 2000: *Prepared for* U.S. Department of Energy, Las Vegas, Nevada, TDR NBSHS 000001 REV 00 ICN 01, 320 p.

CRWMS M&O, 2000b, Commercial spent nuclear fuel degradation in unsaturated drip tests: input transmittal: *Prepared for* U.S. Department of Energy, Las Vegas, Nevada, ACC: DOC: 20000107.0209.

Czerwinski, K. 2007, Technical Report, TR-06-006. "Groundwater Characterization at Yucca Mountain; Task 2: Surface Complexation and Solid Phase Sorption."

Davis, J.A., and Curtis, G.P., 2003, Application of surface complexation modeling to describe Uranium (VI) adsorption and retardation at the Uranium mill tailings site at Naturita, Colorado: U.S. Geological Survey, NUREG/CR-6820, 238 p.

Domenico, P.A., 1987, An analytical model for multidimensional transport of a decaying contaminant species: Journal of Hydrology, v. 91, p. 49-58.

Domenico, P.A. and Schwartz, F.W., 1998, Physical and chemical hydrogeology, 2nd Ed: John Wiley and Sons Inc., New York, 506 p.

Efurd, D.W., Runde, W.H., Banar, J.C., Janecky, D.R., Kaszuba, J.P., Palmer, P.D., Roensch, F.R., and Tait, C.D., 1998, Neptunium and Plutonium solubilities in a Yucca Mountain groundwater: Environment Science and Technology, v. 32, p. 3893-3900.

Haschke, J. M. and Bassett, R. L., 2002, Control of plutonium dioxide solubility by amorphous tetrahydroxide: A critical review of the model: Radiochimica Acta, v. 90, p. 505-509.

Kaplan, D.I., Serkiz, S.M., Fjeld, R.A., and Coates, J.T., 2001, Influence of pH and oxidation state on plutonium mobility through an SRS sediment: WSRC-TR 2001-00472, Rev. O, Westinghouse Savannah River Company, Aiken, S.C.

Kaszuba, J.P., and Runde, W.H., 1999, The aqueous geochemistry of Neptunium: dymaic control of soluble concentrations with applications to nuclear waste disposal: Environment Science and Technology, v. 33, p. 4427-4433.

Kersting, A.B., Efurd, D.W., Finnegan, D.L., Rokop, D.J., Smith, D.K., and Thompson, J.L., 1999, Migration of plutonium in ground water at Nevada Test Site, Nature, v. 397, p. 56-59.

Lemire, R.J. and Tremaine, P.R., 1980, Uranium and plutonium equilibria in aqueous solutions to 200 ºC: Journal of Chemical Engineering Data, v. 25, p. 361-370.

Merkel, B.J. and Planer-Friedrich, B., 2005, Groundwater geochemistry – A practical guide to modeling of natural and contaminated aquatic systems, *Edited by* Nordstrom, D. K.: Springer Berlin Heidelbery, New York, 200 p.

Mitcheltree, W., 2006, Model validation – confidence building by corroboration of PHREEQC and EQ 3/6 model outputs, 2006: *Prepared for* U.S. Department of Energy, DOC: 20061002.009, ANL-EBS-GS-000002 REV 01, 354 p.

Nitsche, H., Gatti, R.C., Standifer, E.M., Lee, S.C., Müller, A., Prussin, T., Deinhammer, R. S., Maurer, H., Becraft, K., Leung, S., and Carpenter, S. A., 1993, Measured solubilities and speciations of neptunium, plutonium, and americium in a typical groundwater (J-13) from the Yucca Mountain region: Los Alamos National Laboratory, Los Alamos, New Mexico, ACC: DOC: 19930507.0136.

Novikov, A.P., Kalmykov, S.N., Utsunomiya, S., Ewing, R.C., Horreard, F., Merkulov, A., Clark, S.B., Tkachev, V.V., Myasoedov, B.F., 2006. Colloid transport of

plutonium in the far-field of the Mayak Production Association, Russia. *Science* 314, 638-641.

OCRWM, 2001, Analysis of geochemical data for the unsaturated zone: *Prepared for* U.S. Department of Energy, ANL-NBS-HS-000017, REV 00, ICN 02, 282 p.

OCRWM, 2003a, Dissolved concentration limits of radioactive elements, June 2003: *Prepared for* U.S. Department of Energy, Las Vegas, Nevada, ANL-WIS-MD-000010 REV 02, 153 p.

OCRWM, 2003b, In-package chemistry abstraction: *Prepared for* U.S. Department of Energy, Las Vegas, Nevada, ANL-EBS-MD 000037 REV 02, ACC: DOC: 20030617.0224, 155p.

Parkhurst, L.D., and Appelo, C.A.J., 1999, User's guide to PHREEQC (Version 2): Water Resources Investigations Report 99-4259.

Rard, J.A., 1997, Potential for radionuclide immobilization in the EBWNFE: solubility limiting phases for Neptunium, Plutonium, and Uranium: Geosciences and Environmental Technologies, Environmental Programs Directorate, Lawrence Livermore National Laboratory, University of California, p. 34.

Runde, W., Conradson, S. D., Efurd, D. W., Lu, N. P. C., VanPelt, E., and Tait, C. D., 2002, Solubility and sorption of redox-sensitive radionuclides (Np, Pu) in J-13 water from the Yucca Mountain site: comparison between experiment and theory: Applied Geochemistry, v. 17, p. 837–853.

Sharp, D.W.A., 1990. *The Penguin Dictionary of Chemistry*, 2nd edition. Penguin Books (London), 434 p.

Viswanathan, H. S., Robinson, B. A., Valocchia, A. J., and Triay, I. R., 1998, A reactive transport model of neptunium migration from the potential repository at Yucca Mountain: Journal of Hydrology, v. 209, p. 251–280.

Wronkiewicz, D.J., Bates, J.K., Gerding, T.J., Veleckis, E., and Tano, B.S., 1992, Uranium release and secondary phase formation during the unsaturated testing of UO_2 at 90 °C: Journal of Nuclear Materials, v. 238, p. 78-95.

Wronkiewicz, D.J. and Buck, E.C., 1999, Uranium mineralogy and the geologic disposal of spent nuclear fuel, *in* Burns, P.C. and Finch, R., eds, Uranium: mineralogy, geochemistry and the environment: Mineralogical Society of America, Washington, DC, p. 475-498.

Windt, L.D., Burnol, A., Montarnal, P., and Lee, J. van der, 2003, Intercomparison of reactive transport models applied to UO_2 oxidative dissolution and uranium migration: Journal of Contaminant Hydrology, v.61, p. 303-312.

Zyvoloski, G., Kwicklis, E., Eddebbarh, A.A., Arnold, B., Faunt, C., and Robinson, B.A., 2003, The site-scale saturated zone flow model for Yucca Mountain: calibration of different conceptual models and their impact on flow paths: Journal of Contaminant of Hydrology, v. 62-63, p. 731-750.

8.2 STANDARDS AND PROCEDURES CITED

University and Community College System of Nevada Quality Assurance Program

QAP-3.1 Control of Electronic Data
QAP-3.3 Models

8.3 SOFTWARE USED

- PHREEQC V. 2.3 (10068-2.3-00 for LINUX, 10068-2.3-01 for WINDOWS 2000)
- Microsoft Excel 2000

8.4 SOURCE DATA, LISTED BY DATA TRACKING NUMBER OR DATA IDENTIFIER

MO0005PORWATER.000. Perm-sample pore water data. Submittal date: 05/03/2000

GS000608312271.001. Pore-water hydrochemistry and isotopic data for boreholes USW NRG-6, USW NRG-7A, USW SD-7, USW SD-9, USW SD-12, USW UZ-14, and UE-25 UZ #16. Submittal date: 01/31/1997

SN0302T0510102.002. Pitzer thermodynamic database. Submittal date: 02/10/2003
SN0504T0502404.011. Pitzer thermodynamic database including actinides and transition metals. Submittal date: 04/19/2005

MO0312SPATHDMIF.000. Thermodynamic data input files – DATA0.YMP.R3. Submittal date: 12/22/2003

R02YL.002 REV 00. Geochemical modeling of solubility and speciation of uranium, neptunium, and plutonium. Submittal date: 09/28/2006

9. ATTACHMENTS

APPENDIX A TRANSPORT MODEL DISCUSSION

A.1 OVERVIEW OF THE TRANSPORT MODEL

Transport of radionuclides in the saturated zone (SZ) depends mainly on (1) the velocity of the groundwater flow (depending on the infiltration rate and distribution of the matrix and fractured rocks), (2) the chemistry of the groundwater (i.e., chemical constituents, oxidation and reduction potential), and (3) physical and chemical properties of rocks (i.e., capability of sorption-desorption) along groundwater the flow path. In this study, the matrix and fracture will be considered together as an effective medium; as a consequence, flow through the fractures of the geological media is not taken into consideration separately.

Based on the geographic condition and groundwater flow direction, the assumed most likely pathway for radionuclides in the transport model to reach the accessible environment is through the uppermost groundwater aquifers below the repository. The accessible environment is determined 20 km down gradient from the repository, where the volcanic rocks pinch out beneath the alluvium fill, and the water table changes gradually from volcanic aquifer to alluvium fill. Therefore the starting point at groundwater table, and then 18 km migration distance in the volcanic tuff, finally 2 km in the alluvium fill are set up in the model.

There are two kinetics reactions within the transport sub-model. One is the element sorption; another is mineral dissolution/precipitation. Each kinetic reaction needs the definition of corresponding rates. The rate expression for mineral dissolution/ precipitation is derived from the example of time-dependent calcite dissolution from Merkel and Planer-Friedrich (2005) and Barnett et al. (2000). The rate expression for element sorption is derived from PHREEQC Manual, Example 15: One Dimensional Transport: Kinetic Biodegradation, Cell Growth, and Sorption. Expression in the keyword RATES in PHREEQC used the mathematics term in the form of BASIC program. For the sorption reaction, the selection of input sorption distribution is based on some references (Moridis et al., 2001; Barnett et al., 2000; Kessler and Doering, 2000; OCRWM, 2003). The bulk density and porosity of rocks are quite different for volcanic and alluvial aquifers, which are set to be 1900 g/L and 0.15, 1270 g/L and 0.3, respectively (Kessler and Doering, 2000).

The transport sub-model is subject to three main restrictions: Firstly, uncertainties lie on transport properties, such as diffusion coefficient, dispersivity coefficient, stagnant cells, and cell distribution. Secondly, two reaction rate expressions for mineral dissolution /precipitation and sorption used for kinetic reaction have the uncertainties considering some parameters, such as activity coefficient, temperature. Thirdly, for the two kinetic reactions used in the transport model, their stoichiometric coefficients, initial moles, and assigned tolerance are the source of uncertainties. The output uncertainty for all the models is summarized in Table 8-2.

Table A-1. Sources of Hydrologic and Thermodynamic Properties Used as Direct Input Data for the Transport Geochemical Model (Some are UQ Data, use for corroboration only).

Source	Data/Parameter Description
Kinetic Data	
LA0010JC831341.005	Kinetic database for sorption reactive transport modeling of uranium
LA0003JC831341.001	Kinetic database for sorption reactive transport modeling of neptunium
LA0010JC831341.006	Kinetic database for sorption reactive transport modeling of plutonium
Kessler and Doering (2000)	K_d of uranium, neptunium, plutonium (UQ data, use for information only)
Geochemistry Data of Groundwater	
GS011108312322.006	Chemical composition of NC-EWDP-19D (alluvium) waters
MO0006J13WTRCM.000	Corroborating chemical composition of water from UE-25 J13 and UE-25 p#1 (carbonate aquifer)

Table A-2. Chemical Components of Solution used in Transport Sub-model (BSC, 2004; BSC, 2003a) (UQ Data, use for corroboration only).

	Solution III	Solution IV	Solution V
Description	Groundwater in volcanic aquifer	Groundwater in alluvium	Groundwater in carbonate aquifer
Na^+ (mg/L)	45	91.5	150
Ca^{2+} (mg/L)	13	3.7	100
Mg^{2+} (mg/L)	2	0.31	39
K^+ (mg/L)	5.3	3.7	12
Cl^- (mg/L)	7.1	6.1	28
SiO_2 (mg/L)	61	22	64.2
HCO_3^- (mg/L)	130	189	694

SO_4^{2-} (mg/L)	18.4	22	160
NO_3^- (mg/L)	N/A	N/A	N/A
F^- (mg/L)	2.2	2.0	N/A

400 cells with length of 46 m each (a total of 18.4 km) are used for the volcanic tuff section. Because groundwater velocity in volcanic tuff is around 46 m/yr (BSC, 2003a), the 46 m is the distance groundwater travel within 1 year, subsequently defined as time step in the simulation. A porosity of 0.065 was selected for fractured network in the volcanic tuff. The hydrodynamic dispersivity of 2 and diffusion coefficient of 5×10^{-11} m^2/s (BSC, 2003c) were selected in the simulation. The boundary condition for this section is defined to be constant hydraulic gradient at the entrance whereas flux at the end (contact point with alluvium).

200 cells with a length of 10 m each (a total of 2 km) are set up for the simulation in the alluvium. The groundwater velocity in the alluvium is approximate 7.5~15 m/yr (BSC, 2003a); the 10 m is the distance that groundwater travels within one year based on the average velocity. So the time step is defined to be 1 year for the simulation as well. An effective porosity of 0.3 was used for kinetic reaction of sorption. A hydrodynamic dispersivity of 5 (BSC, 2003c) was selected in the simulation where the diffusion coefficient is zero (BSC, 2003a). The boundary condition for this section is defined to be flux at the entrance (contact point with volcanic tuffs) whereas constant hydraulic gradient at the end. Moreover, stagnant (immobile) cells were set up with a porosity of 0.1 based on several situ sampling results (BSC, 2004), and an exchange factor of 6.8×10^{-6} (Parkhurst and Appelo, 2000).

A.2 URANIUM TRANSPORT MODEL

The breakthrough curve of total uranium, as well as major aqueous species in the absence of radioactive decay is shown in Figure A-1 where normalized cumulative mass is plotted on the *y*-axis and the time in the unit of years is plotted on the *x*-axis. Based on the information provided by the graphic breakthrough curve, uranium will appear at the 20 km south boundary of waste package after 620 years (after radionuclide entering the SZ). Most of the uranium will be in the form of UO_2CO_3 and $UO_2(CO_3)_2^{2-}$, which is consistent with speciation results provided in Section 6.7.2. This breakthrough curve corresponds to a breakthrough time of total uranium at 50% concentration of 680 years.

The column pattern diagram of uranium transport with sorption reaction is shown in Figure A-2. The uranium sorption versus time curve is shown in Figure A-3. From the sorption curve, the sorption quantity of uranium increases from 640 to 730 years as transported solution passes through alluvial aquifer. Sorption from 750 years falls when the capacity is used up.

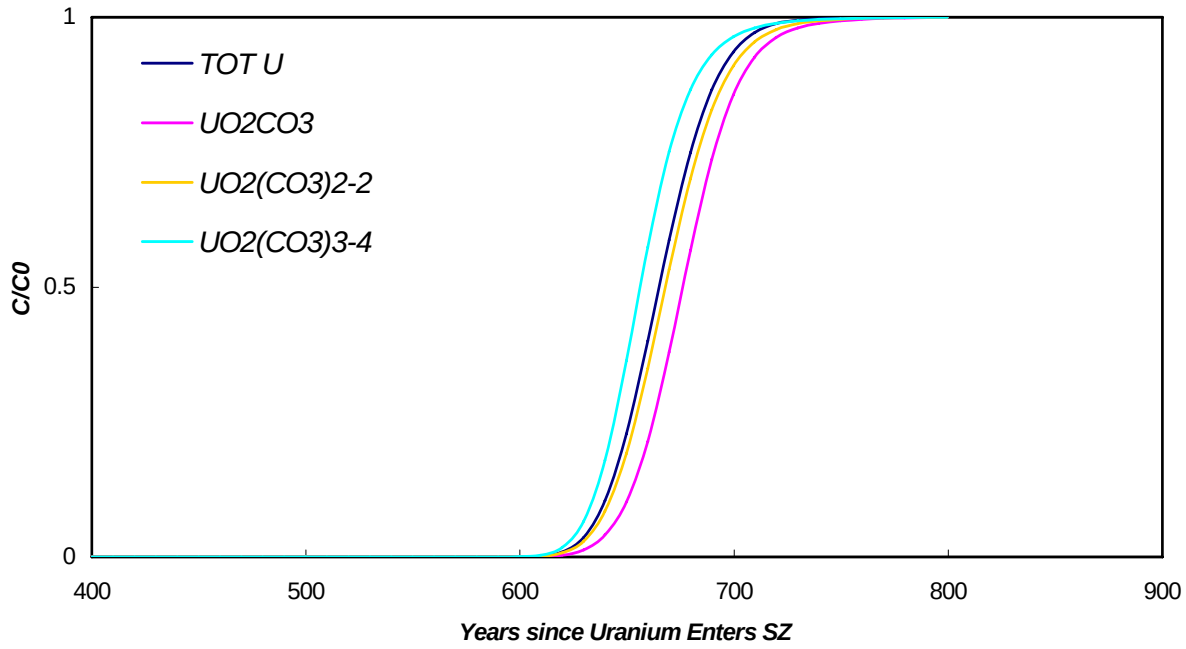

Notes: Mass breakthrough curves and median transport times are for an instantaneous source, present-day climate, and do not include radionuclide decay. The output results are stored in SN: UCCSN-UNLV-087, volume 3

Figure A-1. Breakthrough Curve of Total Uranium and Its Aqueous Species at 20 km South Boundary (UQ Data, use for corroboration only).

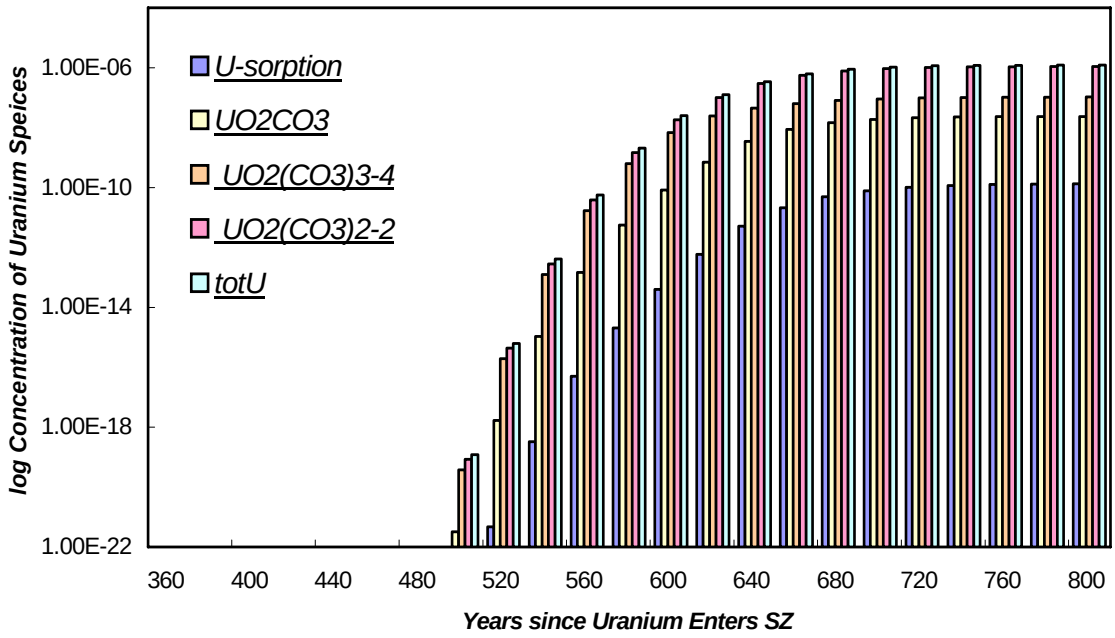

Notes: The output results are stored in Scientific Notebook UCCSN-UNLV-087, vol. 3

Figure A-2. Column Diagram of Uranium Sorption Compares to Uranium Aqueous Species (UQ Data, use for corroboration only).

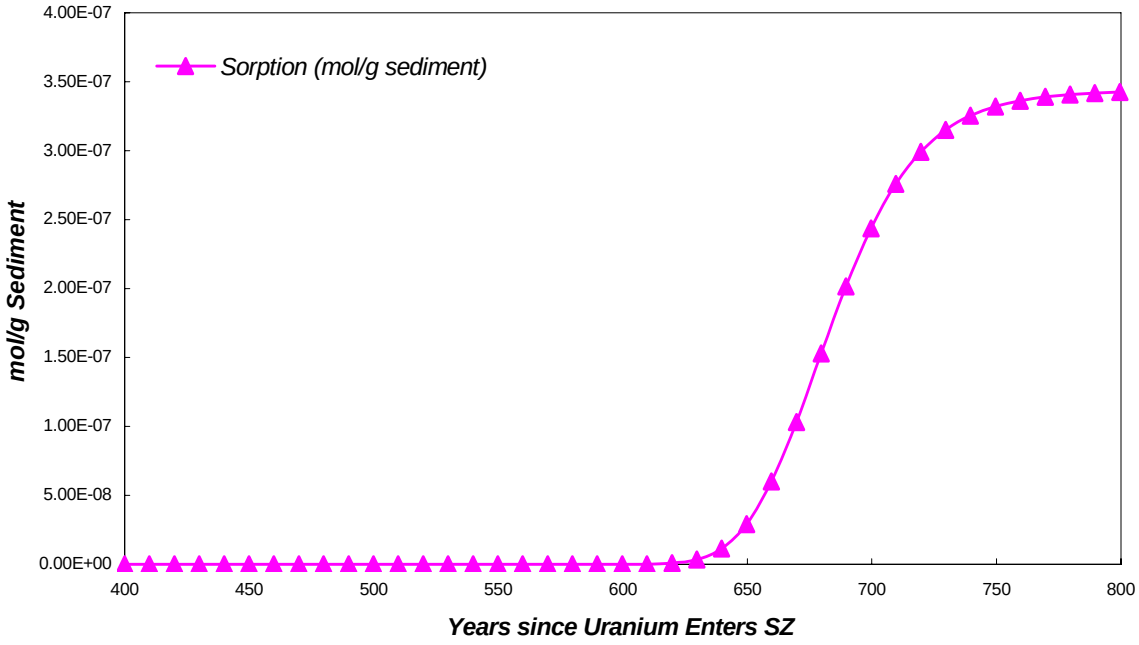

Notes: The output results are stored in Scientific Notebook UCCSN-UNLV-087, vol. 3

Figure A-3. Uranium Cumulative Sorption Activity during Transport Process (UQ Data, use for corroboration only).

A.3 NEPTUNIUM AND PLUTONIUM TRANSPORT MODEL

The breakthrough curve of total neptunium at the simulation boundary with its major aqueous species is shown in Figure A-4. From the plotted breakthrough curve, we can observe that the neptunium species will appear at the 20 km south boundary of waste package after 610 years. Most of neptunium will be in the form of NpO_2^+ and $NpO_2CO_3^-$, which is comparable to the speciation results provided in Section 6.8.2. This breakthrough curve in Figure A-4 corresponds to a breakthrough time at 50% concentration of 660 years.

Figure A-5 plots the plutonium breakthrough curve at the end of alluvium with two dominant aqueous species. The plutonium species will appear after 580 years. Most of plutonium will be in the form of $Pu(OH)_4$, which is in agreement with speciation results of Section 6.9.2. This breakthrough curve corresponds to a breakthrough time at 50% concentration of 620 years.

The sequence of actinide appears at 20 km simulation boundary, from first to last, would be plutonium, neptunium, and uranium. The various breakthrough times indicates the different impacts of sorption reactions between individual elements and the surrounding geological material. Even though plutonium has a relative larger sorption coefficient than that of neptunium and uranium, the total sorption quantity is less than these for neptunium and uranium because of much lower solution concentration of plutonium. The assigned sorption coefficients of neptunium and uranium are quite close to each other, however, the total sorption quantity of uranium is more than that of neptunium, because its overall higher solution concentration. These results are consistent with the breakthrough curves of Base Case, conservative, and sorbing radionuclides in the absence of radioactive decay from BSC (2004).

The molar of neptunium sorption quantity per gram of surrounding rocks through time is plotted in Figure A-6. The sorption quantity of neptunium increases rapidly between 650 to 720 years and then turns stable after 750 years. Compared to the uranium sorption curve and different solution concentrations of these two elements, neptunium has a weaker affinity to the surrounding rocks than uranium.

Figure A-7 shows the molar of plutonium sorption quantity per gram of surrounding rocks versus time. Even the distribution coefficient of plutonium is about 20 times larger than those of uranium and neptunium; the sorption curve doesn't show a higher sorption quantity, yet much lesser, than uranium and neptunium. This is mainly due to the low solution concentration of plutonium solution, which is only 3×10^{-10} mol/L. Also, the sorption curve of plutonium has the different pattern as those of uranium and neptunium, where the sorption quantity has kept increasing since 600 years after it enters SZ. This is caused by low solution concentration of plutonium available for sorption reaction, thus still leaving sufficient area of surrounding rock available for sorption.

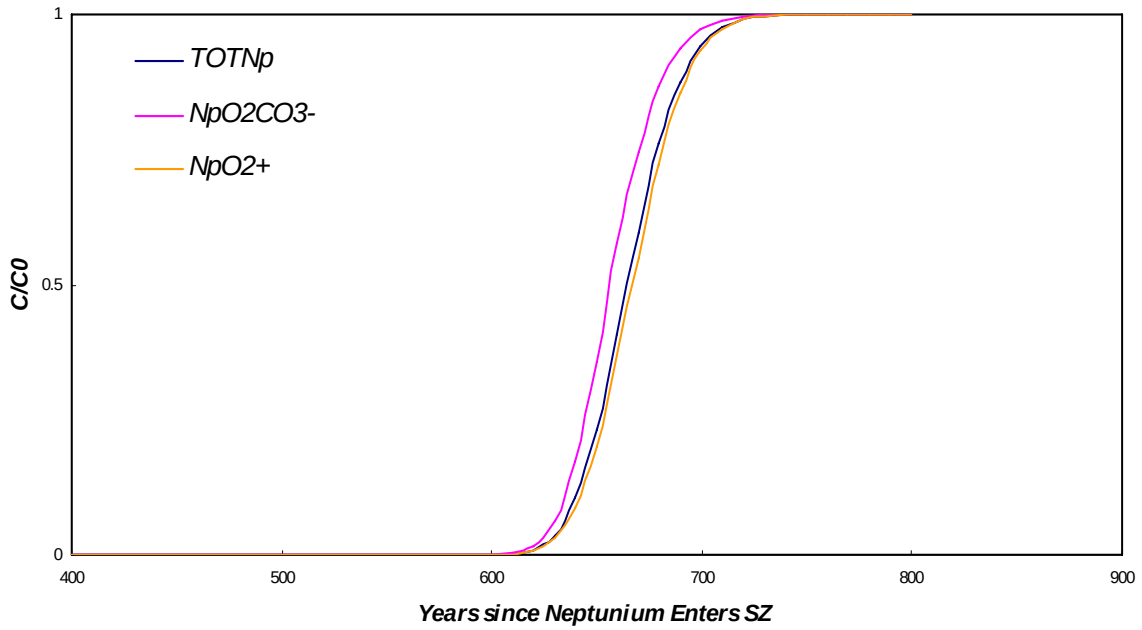

Notes: Mass breakthrough curves and median transport times are for an instantaneous source, present-day climate, and do not include radionuclide decay. The output results are stored in Scientific Notebook: UCCSN-UNLV-087, vol. 3.

Figure A-4. Breakthrough Curve of Neptunium in Alluvium Aquifer (UQ Data, use for corroboration only).

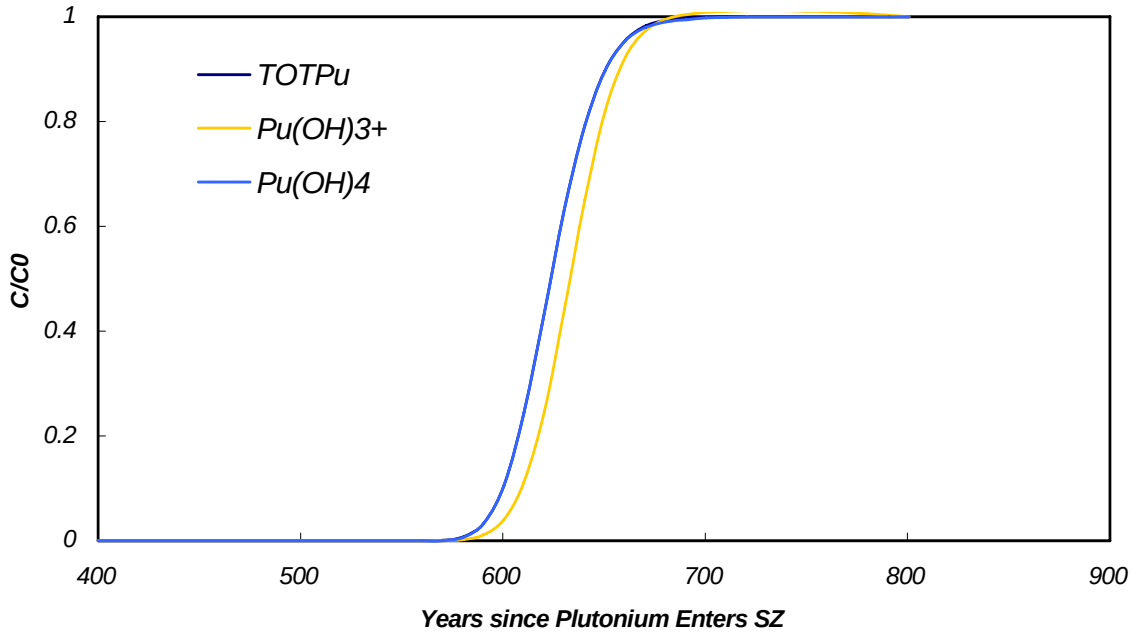

Notes: Mass breakthrough curves and median transport times are for an instantaneous source, present-day climate, and do not include radionuclide decay. The output results are stored in Scientific Notebook: UCCSN-UNLV-087, vol. 3.

Figure A-5. Breakthrough Curve of Plutonium in Alluvium Aquifer
(UQ Data, use for corroboration only).

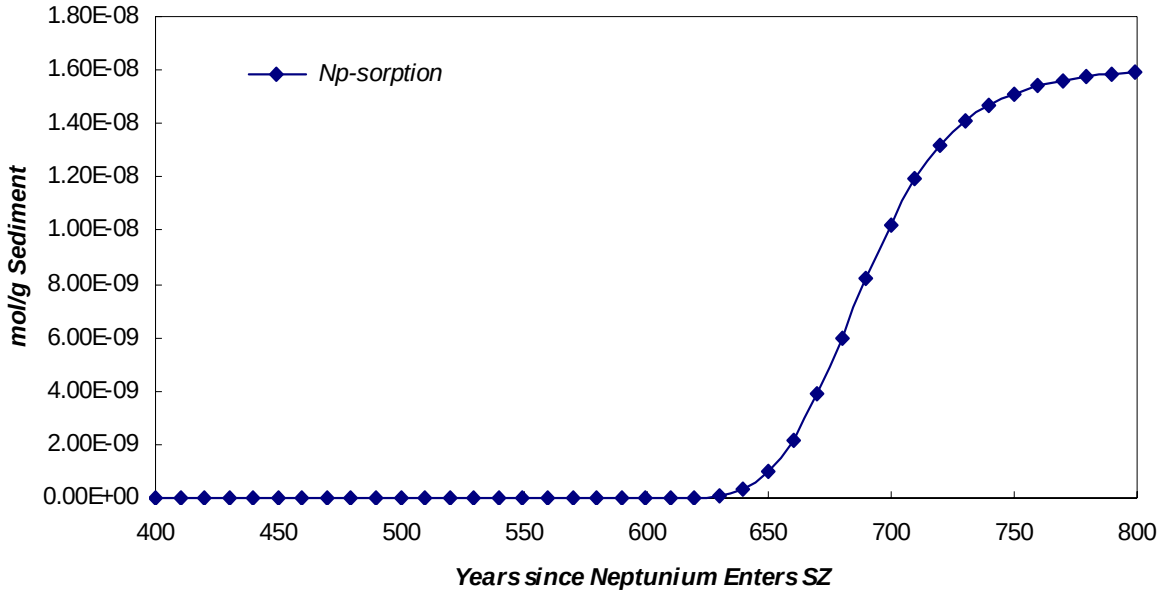

Notes: The output results are stored in Scientific Notebook UCCSN-UNLV-087, vol. 3.

Figure A-6. Neptunium Cumulative Sorption Activity during Transport Process
(UQ Data, use for corroboration only).

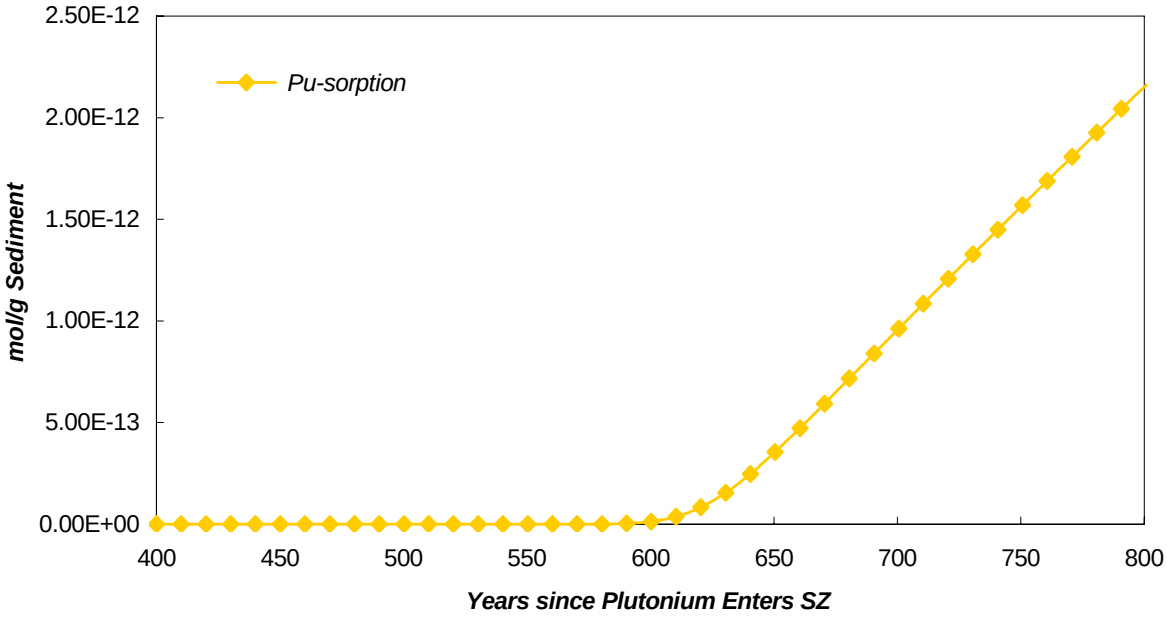

Notes: The output results are stored in Scientific Notebook UCCSN-UNLV-087, vol. 3.

Figure A-7. Plutonium Cumulative Sorption Activity during Transport Process
(UQ Data, use for corroboration only).

REFERENCES FOR APPENDIX A

Barnett, M.O., Jardine, P.M., Brooks, S.C., and Selim, H.M, 2000, Adsorption and transport of uranium (VI) in subsurface media: Soil Science Society of America Journal, v. 64, p. 908-917.

Bechtel SAIC Company, 2004, Site-scale saturated zone transport, November 2004: *Prepared for* U.S. Department of Energy, MDL-NBS-HS-000010 REV 02, 366 p.

Bechtel SAIC Company, 2003a, Saturated zone flow and transport, Revision 2, September 2003: *Prepared for* U.S. Department of Energy, 402 p.

Bechtel SAIC Company, 2003b, Geochemical and isotopic constraints on groundwater flow directions and magnitudes, mixing, and recharge at Yucca Mountain, July 2003: *Prepared for* U.S. Department of Energy, ANL-NBS-HS-000021 REV 01, 505 p.

Bechtel SAIC Company, 2003c, Saturated zone flow and transport model abstraction, July 2003: *Prepared for* U.S. Department of Energy, MDL-NBS-HS-000021 REV0, 195 p.

Kessler, J. and Doering, T., 2000, Evaluation of the candidate high-level radionuclides waste repository at Yucca Mountain using total system performance assessments: Phase 5 (1000802), Electronic Power Research Institute, Palo Alto, CA, 94304.

Merkel, B. J. and Planer-Friedrich, B., 2005, Groundwater geochemistry – A practical guide to modeling of natural and contaminated aquatic systems, *Edited by* Nordstrom, D. K.: Springer Berlin Heidelbery, New York, 200 p.

Moridis, G.J., Hu, Q., Wu, Y.S., and Bodvarsson, G.S., 2001, Preliminary 3-D site scale studies of radioactive colloid transport in the unsaturated zone at Yucca Mountain, Nevada: Earth Sciences Division, Lawrence Berkeley National Laboratory, 57 p.

OCRWM, 2003, Saturated zone flow and transport model abstraction, August 2003: Office of Civilian Radioactive Waste Management, Las Vegas, Nevada, MDL-NBS-HS-000021 REV 00, 195 p.

Parkhurst, L.D., and Appelo, C.A.J., 1999, User's guide to PHREEQC (Version 2): Water Resources Investigations Report 99-4259.

LA0010JC831341.005. Radionuclide retardation measurements of sorption distribution coefficients for uranium. Submittal date: 10/19/2000

LA0003JC831341.001. Radionuclide retardation measurements of sorption distribution coefficients for neptunium. Submittal date: 10/19/2000

LA0010JC831341.006. Radionuclide retardation measurements of sorption distribution coefficients for plutonium. Submittal date: 10/19/2000

LA0302MD831341.004. Uranium sorption in alluvium from NC-EWDP wells 191M1A, 10SA, and 22SA under ambient conditions. Submittal date: 02/11/2003

MO0006J13WTRCM.000. Recommended mean values of major constituents in J-13 well water. Submittal date: 06/07/2000